



FACULTY OF SCIENCE AND TECHNOLOGY

BACHELOR THESIS

Study programme / specialisation: Kjemi og Miljø, Biologisk Kjemi

The spring semester, 2022

Open

Authors: Mathias Sandvik, Nikolai Ersdal

.....
...

.....
...

Course coordinator: Emil Lindbäck

Authors Signatures:

Supervisor: Emil Lindbäck

Thesis title: "A Complete Synthesis of an N-spirofused Iminosugar from L-xylose; a Potential Cholinesterase Inhibitor for Treatment of Alzheimer's Disease"

Credits (ECTS): 20

Keywords: Alzheimers Disease, Cholinesterase, Cholinesterase Inhibitor, Iminosugar, acetylcholine, L-Xylose, 3.2.6 (1R,2R,3R)-2,3-bis(benzyloxy)-1-[(benzyloxy)methyl]-5-azoniaspiro [4.4] nonane.

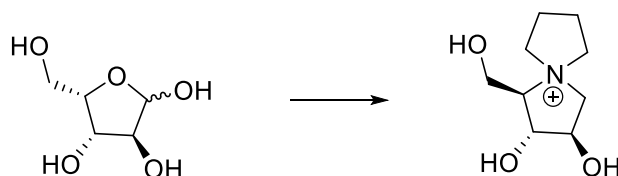
Pages: 36 + appendix: 7

Stavanger, 15.05.2022

University of Stavanger

BACHELOR'S THESIS

A complete synthesis of an N-spirofused iminosugar from L-xylose; a potential cholinesterase inhibitor for treatment of Alzheimer's disease



Co-Authored by:

Nikolai Ersdal & Mathias Sandvik

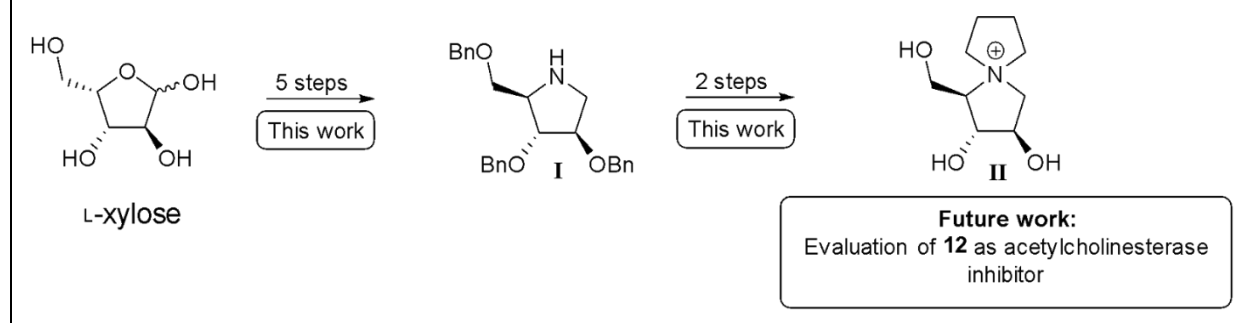
Supervised by:

Emil Lindbäck

Department of Chemistry, Bioscience and Environmental Engineering

- 15.05.2022

Graphical Abstract



Abstract

In this bachelor's project we present a complete synthesis of an *N*-spirofused iminosugar **II**¹ with a stable positive charge on the spirocyclic nitrogen atom that together with the hydroxyl groups are expected to establish interactions with the residues in the active gorge of the acetylcholinesterase. Compound **II** was successfully synthesized through seven steps from commercially available L-xylose at an overall yield of 3%. This was done through the strategy of initiating an S_N2 cyclisation on pyrrolidine **I**, thereby creating the *N*-spirofused bicyclic iminosugar, before finally removing the protection groups.

¹ Roman numerals refer to the compounds in the graphical abstract

Acknowledgements

Isaac Newton famously wrote that we as scientists stand on the shoulders of giants as a metaphor for our work being based on the understanding gained by our predecessors. This is not completely right, as giants imply a few larger-than-life thinkers rather than the fact that all our work is not based on a few pieces of, but a mountain of evidence, work and effort made by an uncountable number of scientists whose names are never going to decorate textbooks, maps, or museums. Neither are the names of the people donating their organs and funds in the pursuit of that knowledge nor the teachers who taught all the basics or the ones who again assisted them. The point here being that any work is a collective achievement of all those who made that work possible directly, or indirectly.

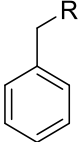
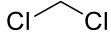
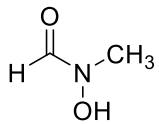
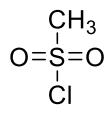
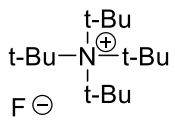
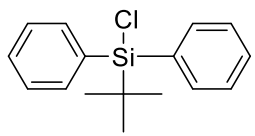
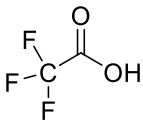
As there are more of these people assisting from the shadows than there is room on this one page, a big thank you goes out to all of our loved ones, teachers and friends helping us with producing our own little kernel of knowledge to be placed on the glorious mountain of science

We would also like to specifically thank our supervisor Emil for the trust, time, and energy he manages to pull out of what seems like thin air in his very busy life. We couldn't ask for a better supervisor who has made the lab and meetings a reason to jump out of bed every morning of the project. We would also like to thank you for creating an atmosphere of teamwork we are sad to now see the end of. Thank you so much for all the laughs and learnings.

Another special thanks must be awarded to Anisha M. Butt for her generous offerings of equipment and helpful assistance without ever complaining about the incompetent bachelor students, making a mess of her lab.

Caroline Vaaland, Marianne Bore Haarr, Katja Håheim, Ananya Chari and Erling B. Monsen should also be highlighted as people who stopped everything they were doing, no matter their schedules, to help the bachelor students not blow up the faculty building.

Selected Abbreviations

Abbreviation	Full name	Structure (chemical)
AChE	Acetylcholinesterase	
APP	Amyloid precursor protein	
Bn	Benzyl	
BuChe	Butylcholinesterase	
CAS	Catalytic anionic site	
DCM	Dichloromethane	
DMF	<i>N, N</i> Dimethylformamide	
FCC	Flash Column Chromatography	
NMDA	<i>N</i> -methyl-D-aspartate	
MsCl	Mesylchloride	
PE	Petroleums Ether	
PAS	Peripheral anionic site	
Rf	Retardation factor	
TBAF	tert-butylammoniumfluoride	
TBDPSCI	tert-butyl(chloro)diphenylsilane	
TFA	Trifluoroacetic acid	

Contents

1 Introduction 1

- 1.1 Alzheimer's disease 1
- 1.2 Neuropathology 2
 - 1.2.1 Amyloid Hypothesis 3
 - 1.2.2 Cholinergic Hypothesis 3
 - 1.2.3 Cholinesterases 4
- 1.3 Current FDA Approved Treatments 5
- 1.4 Iminosugars 7
- 1.5 Objectives 9

2 Results and discussion 10

- 2.1 *Synthesis of N-spirofused Iminosugar* 10
 - 2.1.1 *O-Benzoylation of L-xylose* 10
 - 2.1.2 *Addition of Aminehydroxyl and Regiospecific O-silylation to Protected Methyl-L-xylofuranoside* 12
 - 2.1.3 *O-Mesylation of Silyl Protected Oxime* 14
 - 2.1.4 *Formation of Zwitterionic N-Oxide by Addition Elimination Through Pentacoordinated Intermediate* 15
 - 2.1.5 *Reduction of N-C double bond by NaBH₄ and Zn* 16
 - 2.1.6 *Synthesis of N-spirofused bicyclic Iminosugar by S_N2 cyclization* 17
 - 2.1.7 *Benzyl Group Deprotection of N-spirofused Iminosugar* 18
- 2.2 *Concluding Remarks and the Future of AChE Inhibitors* 19

3 Experimental 21

- 3.1 Practical 21
 - 3.1.1 Solvents and Reagents 21
 - 3.1.2 Spectrometric and Spectroscopic Analysis 21
 - 3.1.3 Chromatography 21
- 3.2 Experimental 22
 - 3.2.1 *Methyl 2,3,5-Tri-O-benzyl-L-xylofuranose* 22
 - 3.2.2 *(2R,3R,4S, E)-2,3,5-Tris(benzyloxy)-4-hydroxypentanal O-(tert-butyl-diphenylsilylchloride) oxime* 23
 - 3.2.3 *2,3,5-Tri-O-benzyl-4-methanesulfonyl-L-xylofuranose Oxime* 24
 - 3.2.4 *(2R,3R,4R)-3,4-Bis(benzyloxy)-2-((benzyloxy)methyl)-3,4-dihydro-2H-pyrrole 1-oxide* 24
 - 3.2.5 *(2R,3R,4R)-3,4-bis(benzyloxy)-2-[(benzyloxy)methyl]-1H-pyrrolidine* 25
 - 3.2.6 *(1R,2R,3R)-2,3-bis(benzyloxy)-1-[(benzyloxy)methyl]-5-azoniaspiro [4.4]* 26
 - 3.2.7 *(1R,2R,3R)-2,3-Dihydroxy-1-(hydroxymethyl)-5-azoniaspiro [4.4] nonane* 26

4 References 27

5 Appendix 30

1.0 Introduction

1.1 Alzheimer's disease

Alzheimer's disease (AD) is a neurodegenerative disease that is most common cause of dementia. AD is approximated to account for 60-80% of all dementia cases worldwide.

The greatest risk factor of Alzheimer's is aging as the disease is most common in people 65 years and older. There are cases where younger people are affected with AD, known as early onset-AD, however this is not as common. AD is a devastating irreversible disorder in which regions of the brain that are responsible for the cognitive functions undergo gradual shrinkage due to neuronal loss³⁰ before death occurs ca 4-8 years after diagnosis¹. and the dementia it causes are terrible diseases where the brain, dies slowly before the body it controls. This is extremely traumatic not only for the patient slowly losing control over themselves, but also for their immediate family and friends losing their loved one piece by piece. First symptoms appear as difficulty learning new skills and information, then disorientation, mood swings, confusion, memory loss, difficulty speaking eventually leading to struggles with swallowing and walking¹. A person with severe AD will require assistance to live a normal life.

As of 2020 there were reported to be 55 million people suffering from AD worldwide, a number which is predicted to double every 20 years due to aging populations as a result of advancements in technologies. The combined costs of medicine, healthcare and lost human resources on a global scale was approximated to be worth 1.3 trillion USD, a sum which is predicted to double by 2030.² At the moment of writing, 80-100 thousand people are estimated to be living with dementia in Norway³. If one were to assume that all AD patients are to receive an equal size of the economic estimate, that means that the economic impact on Norway alone is 1.2-2.08 billion USD. The upper limit of that estimate would be equal to 0,5% of total GDP in 2022.

Despite being a disease over 100 years old with enormous social, economic, and worldwide impact, AD does still not yet have any established cure, therapy, nor any treatments capable of slowing disease progression¹.

1.2 Neuropathology

AD is a neurodegenerative disorder characterized by neuritic plaque and neurofibrillary tangle buildup in the brain. This plaque is visible in the temporal lobe and neocortical structures of AD brain (**Figure 1**)¹. For a diagnosis to be given, a patient must undergo a series of tests including Neurological examination, magnetic resonance imaging (MRI) of the brain, B12 level lab tests, as well as a family history questionnaire to determine heredity. True AD diagnoses however can only be given after examination under autopsy where a histopathologic confirmation can be made through the discovery of the large plaques and massive loss of neurons similar to the ones found by Alois Alzheimer in the first documented AD patient in the early 1900s⁵.

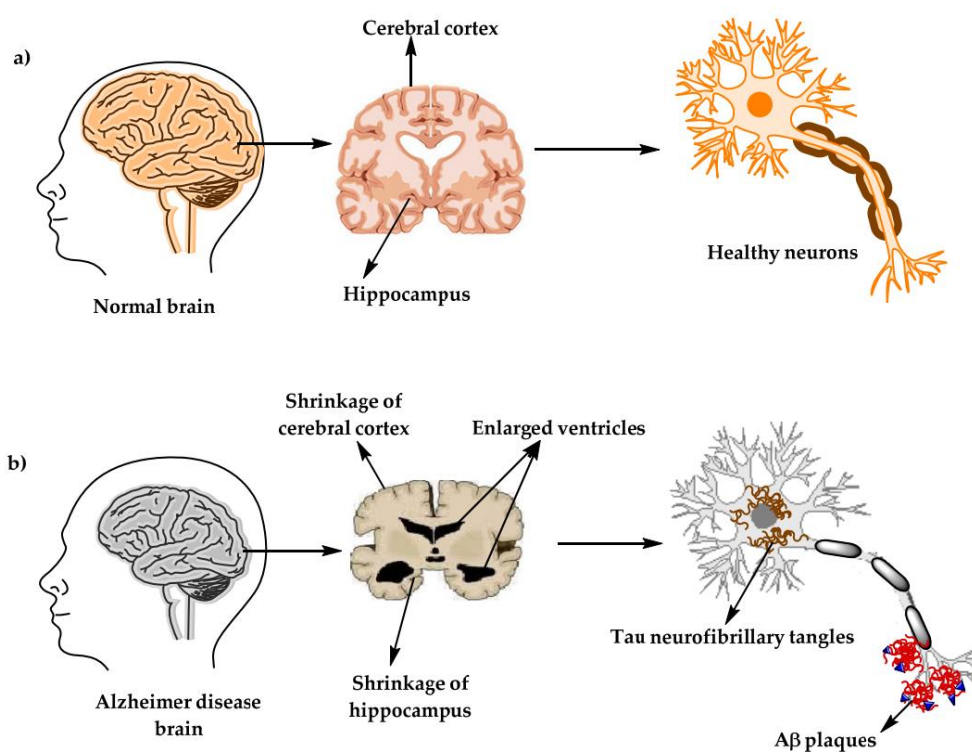


Figure 1 - The physiological structure of the brain and neurons in (a) healthy brain and (b) AD brain⁵

What causes AD is not yet understood but scientist agree on two main hypotheses⁵. The primary source of ideas stems from the Amyloid and Cholinergic Hypotheses.

1.2.1 Amyloid Hypothesis

The Amyloid cascade hypothesis is based on the theory that mutations in PS1 or PS2 genes increases production and accumulation or decrease the catabolism of amyloid-beta(A β) proteins from the hydrolysis of amyloid precursor protein (APP) or decreasing its catabolism. This leads to the binding of A β proteins as oligomers in the brain and causes abnormal deposits of plaques and interfering with cellular signaling. Amyloid plaques also accumulate in healthy aging however not in the levels seen in AD.

These A β oligomers block and interact with the synapses which through a set of complex mechanisms leads to progressive synaptic and neuritic damage. This again causes changes to the neural ionic homeostasis and oxidative injury which again leads to altered enzyme activity and ultimately neural cell death causing loss of brain function. On the outside this will be observed as symptoms of dementia^{5,6}.

There is more to discuss concerning the accumulation of Beta-amyloid and Tau-proteins in AD brain, the evolution of the hypothesis and its general correlations with AD. However, as the target molecule of this paper is not predicted to target or interact with any of the relevant mechanisms. Further delving into the amyloid hypothesis is considered beyond the scope of this paper.

1.2.2 Cholinergic Hypothesis

The biochemical investigation behind the cause of AD began already in the late 1960s over 50 years from today. Already in the mid-70s there was discovered deficits in the enzyme responsible for the synthesis of acetylcholine (ACh) choline acetyltransferase (ChAT) as well as choline uptake and ACh release indicated a large cholinergic deficit in AD⁷. This is also when the link between ACh, learning and memory was discovered. All this information led to the Cholinergic hypothesis.

The hypothesis stipulates that degeneration of the cholinergic neurons in the basal forebrain and therefore the loss of cholinergic neurotransmission in the cerebral cortex and other parts

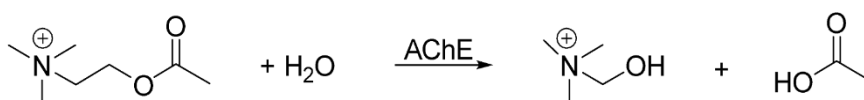
of the brain led to the deteriorative neural state in patients suffering from AD. Later studies have shown that this does not cause cognitive decline directly as much as indirectly but did provide the theory that acetylcholinesterase-inhibitors(AChEIs) like the target molecule of this paper would slow down the symptoms of AD which turned out to be correct⁷.

So the three factors of the cholinergic hypothesis are:

- 1: less cholinergic substrates in AD brain.
- 2: Severe neurodegeneration in the basal forebrain region of the brain.
- 3: The role of cholinergic promoters as opposed to their antagonists⁵.

1.2.3 Cholinesterases

The primary antagonist of ACh is acetylcholinesterase (AChE) which catalyzes the hydrolysis of ACh (**Scheme 1**) in its active gorge thereby metabolizing neural signaling substrate, which in AD patients are already lacking (*vide supra*). AChE is located in neural postsynaptic junctures and serves the primary function of inhibiting spreading of ACh to nearby synapses in healthy individuals⁸.



Scheme 1 - The hydrolysis reaction of ACh catalyzed by AChE

Another cholinesterase (ChE) is butyrylcholinesterase (BuChE) primarily excreted from glial cells as opposed to neurons, the enzyme seems to fulfill the same functions as AChE but are way less prominent until the onset of AD where the enzyme proliferates in higher numbers as the disease progresses⁹.

The catalytic triad in the catalytic anionic site (CAS) of active gorge of AChE is where the hydrolysis of ACh takes place (**Figure 2**). Tryptophan acts as an anionic subunit of CAS making it susceptible for Cationic interactions whereas the peripheral anionic site (PAS) serves as a guide for appropriate AChs. This active gorge is the target of the molecule of interest in this paper (Figure 2)¹⁰.

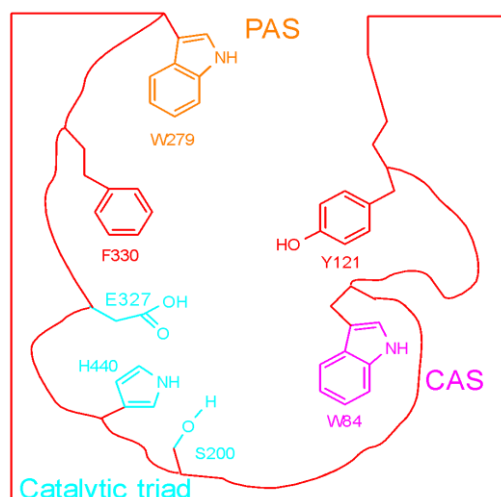


Figure 2: The active gorge of AChE

1.3 Current FDA Approved Treatments

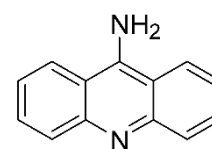
Although a mountain of scientific effort has been put on finding the causes and cure against AD, nothing other than theories and palliative treatments have been discovered at the moment of writing. However, newer promising treatments have been arriving on the market one after another.

1.3.1 Tacrine

The first drug approved by the FDA for treatment of AD was Tacrine.

Tacrine was a cholinesterase inhibitor intended to increase the bioavailability of ACh by preventing its metabolism. It showed promising but not amazing results. Due to its hepatotoxicity affecting approximately

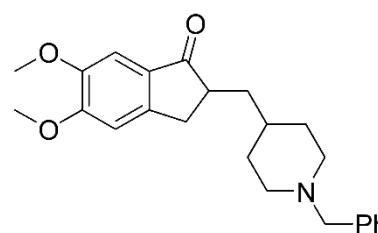
25% of the users, tacrine got discontinued from clinic use in 2013. However, tacrine is still an attractive moiety in the development of new AChE inhibitors, and many such derivatives have been tested both in *vitro* and *vivo*^{11,12}.



1 Tacrine

1.3.2 Donepezil

Donepezil FDA approved in 1996 is another cholinesterase inhibitor used in the treatment of AD and other forms of dementia. Unlike tacrine it is only rarely linked to liver toxicology, but does show side effects such as insomnia, nausea, loss of appetite, diarrhea, and muscle weakness. It is

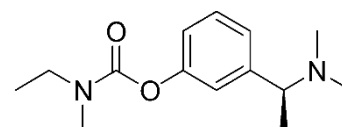


2 Donepezil

not reported to reverse or halt the progression of the disease, but it delays the symptoms by a few months for patients suffering from moderate and severe AD. Additionally Donepezil is extremely selective towards AChE over BuChE and has also spawned the research of derivatives retarding A β plaque generation^{11,13,22}.

1.3.3 Rivastigmine

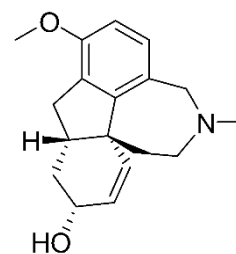
Rivastigmine FDA approved in 2000 is a reversible cholinesterase inhibitor meaning it can easily dissociate from the enzyme. Like donepezil it does not display a high prevalence of liver toxicity, however it presents other major side effects such as stomach pain, weight loss, diarrhea, nausea, vomiting and loss of appetite. Rivastigmine exhibits dual AChE/BuChE inhibitory activity and is only recommended for patients suffering from mild to moderate cases of AD. Donepezil does not slow disease progression but only treats symptoms. Interestingly Rivastigmine shows higher affinity to one of the isoforms of AChE, which appears to increase in prevalence in the progression of AD, this has sparked research in derivatives, which show even higher activity. In Rat trials Rivastigmine has also shown higher concentration of APP, implying that it also reduces the buildup of A β ^{11,14,22}.



3 Rivastigmine

1.3.4 Galantamine

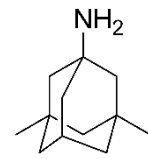
FDA approved in 2001, galantamine is a reversible, competitive inhibitor of AChE. In addition to blocking the breakdown of ACh, galantamine is an allosteric modulator of the nicotinic receptors which are prototypical, ligand-gated ion channels that assist in fast cell signaling in the nervous systems, thereby having two mechanisms of medical significance in AD patients. Galantamine shows no correlation with hepatotoxicity but has been associated with side effects like convulsions, severe nausea, stomach cramps, vomiting, irregular breathing, confusion, muscle weakness and watering eyes. Galantamine is recommended in mild to moderate cases of AD and again does not slow disease progression, but only treats symptoms. Galantamine also increases serotonin and glutamate bioavailability, the latter of which is another important neural signaling molecule^{11,15,22}.



4 Galantamine

1.3.5 Memantine

FDA approved in 2003 memantine is not a AChE inhibitor, but low affinity uncompetitive *n*-methyl-D-Aspartate (NMDA) receptor antagonist which binds preferentially to the NMDA receptor-operated cation channels, thereby blocking the effect of glutamate, a neurotransmitter which in high doses can lead to overstimulation and excessive signaling which again can lead to oxidative neural stress and hyperactivity of the glutamate receptors and cell death in the brain of AD patients. It also shows no link to liver toxicology and is used in treatment of moderate to severe cases of AD. As memantine targets another mechanism trials that investigate combining it with donepezil have concluded that it has positive effects, however the burden of multiple medications and the risk of negative synergistic effects makes researchers skeptical of the treatment. Side effects associated with memantine include dizziness, confusion, aggression, depression, headache, sleepiness, diarrhea, constipation, nausea, vomiting, weight gain, bodily pains and cough^{11,16,17,22}.



5 Memantine

1.3.6 Aducanumab

Aducanumab has been considered as a controversial medicine due to its rushed rollout through the FDA in 2021 without full confirmation of efficacy in all the various clinical trials. Aducanumab is also the only drug approved for AD that has been able to show a reduction of amyloid-plaques in AD brain like discussed in the amyloid hypothesis. Scientists are in hot discussion of whether plaques are the right thing to target in AD, as only one of the clinical phase three trials showed moderately positive results in mild cases of AD the others showing no or negative results. Around 40% of patients in the trials also developed brain swelling requiring brain scans. Although no symptoms were reported this causes additional strain on the health care systems. Biogen will charge 56'000 dollars a year for the drug which will make this the most expensive treatment for AD thus far. Aducanumab is a whole antibody meaning it is not a chemical like the other drugs currently available on the market^{18,19}.

1.3.7 Iminosugars

Iminosugars are monosaccharide analogues in which the ring oxygen has been replaced by a nitrogen atom. The nitrogen substitute allows for both increased polarity and additional

stereochemistry as opposed to its group 16 and 14 counterparts²⁰.

Two examples of iminosugars are 1-deoxynojirimycin (**X**) and 1,4-dideoxy-1,4-imino-D-arabinitol (**Y**).

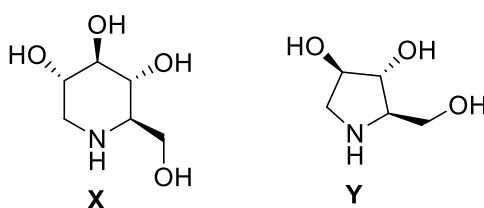


Figure 3 - Display of 1-deoxynojirimycin (X) and 1,4-dideoxy-1,4-imino-D-arabinitol (Y)

Iminosugars are mostly famous for their properties as glucosidase inhibitors. Therefore, iminosugars are attractive lead-compounds for treatment of diseases such as Gaucher's disease, type 2 diabetes, HIV and cancer, which involve carbohydrate processing enzymes. It has also been discovered that some iminosugars can act as potent AChEIs similar to the intended biochemical role of most current AD medication. This is possible due to the chemical similarities between iminosugars in their protonated form and ACh.²¹

1.4 Objectives

The objective of this bachelor thesis will be to synthesize *N*-spirofused iminosugar **12** as an AChE inhibitor candidate. The positively charged nitrogen atom is envisaged to establish cation- π -interactions with the tryptophan residue in the (CAS) region. In addition, the hydroxyl groups are expected to generate hydrogen bonds with the residues in the catalytic triad of the enzyme.

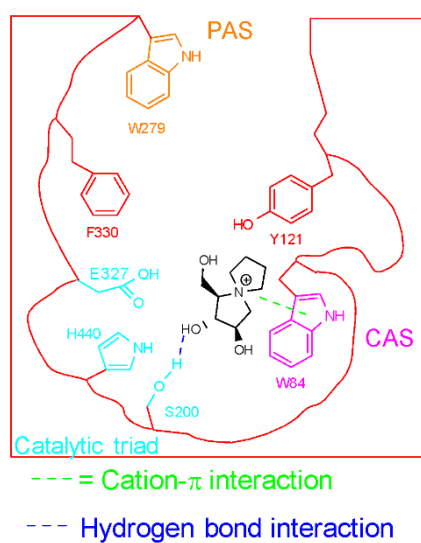
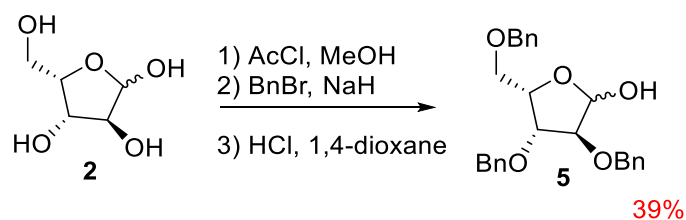


Figure 4 - 2d model of active gorge with Target molecule added, with lines, indicating the gorge-molecule interactions. Model is based on data from reference 31

2.0 Results and discussion

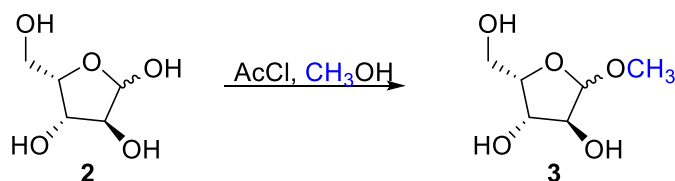
2.1 Synthesis of *N*-spirofused iminosugar

2.11 *O*-Benzylation of L-xylose



Scheme 2 - O-Benzylation of L-xylose

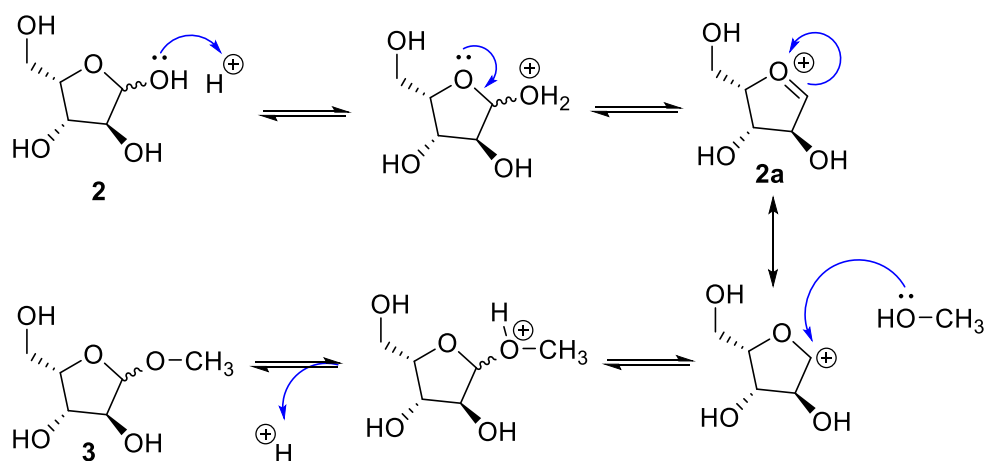
To provide orthogonal protection on the anomeric hydroxyl group in L-Xylose (**2**), a methyl group was added using a Fisher glycosylation method to provide an anomeric mixture of methyl-L-xylofuranoside (**3**) (**Scheme 2**).



Scheme 3 - Fisher glycosylation of L-Xylose

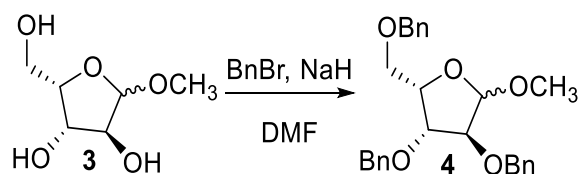
This orthogonal protecting group was added due to its simple removal and to inhibit benzylation of the anomeric hydroxyl group. In the following step, acetyl chloride was used to generate an acid catalyst (HCl) in situ when it reacts with methanol ($\text{MeOH} + \text{AcCl} \rightarrow \text{HCl} + \text{NaOMe}$).

The acid catalyst attacks the anomeric hydroxyl group to eliminate water, thereby creating an oxocarbenium ion **2a** that is resonance stabilized with the corresponding glycosyl cation (**Scheme 4**). Lone pair electrons from methanol initiates a nucleophilic attack to insert a methyl group and recycle the acidic proton by electron rearrangement to give the glycosylated L-xylose **3** (**Scheme 4**).



Scheme 4 - Suggested mechanism on Fisher glycosylation

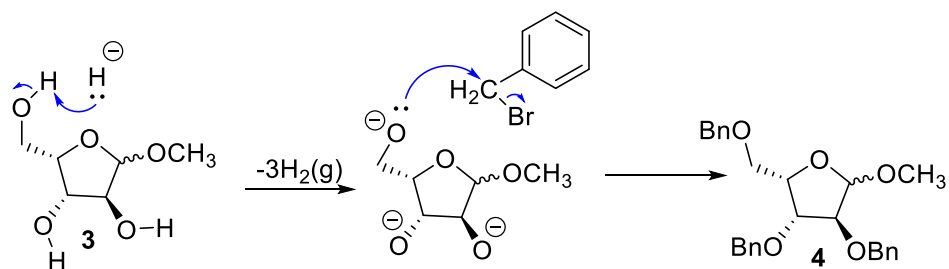
Next, the remaining hydroxyl groups in methyl furanoside **3** were protected by *O*-benzylation upon treatment with NaH and BnBr in DMF to provide the perbenzylated methyl alpha-*L*-xylofuranoside **4** (Scheme 5).



*Scheme 5 - O-Benzoylation of methyl-*L*-xylofuranoside*

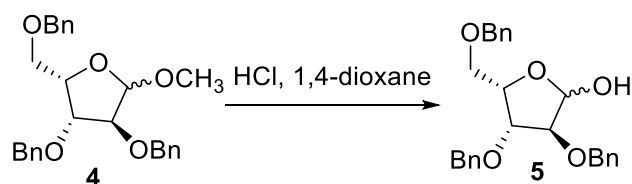
The choice to protect by *O*-benzylation was preferable due to the mild condition requirements to install and remove the Bn-groups using palladium-catalyzed hydrogenation. Alternatively, one could use acetyl groups as global protecting groups. However, the deprotecting procedures are generally easier for benzyl groups and global *O*-benzylation was therefore preferred.

The mechanism provided in Scheme 5 suggests that NaH deprotonates the hydroxyl group making it possible for a nucleophilic attack by the oxygen to the benzyl group simultaneously expelling the bromide group in an S_N2 fashion.



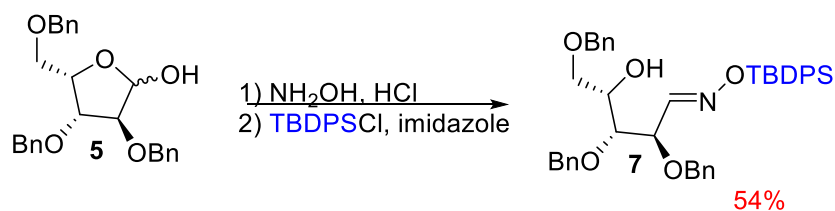
Scheme 6 - Suggested mechanism of O-Benzylation of methyl-L-xylofuranoside²⁸

The methyl group furanoside **4** is finally removed by using aqueous HCl at elevated temperatures using the reverse mechanism that went under Fisher glycosylation protocol in the first step. The product of protected L-xylose **5** was purified by silica column chromatography to provide a 39% yield over three steps (Fisher glycosylation, benzylation and hydrolysis of glycosidic bond).



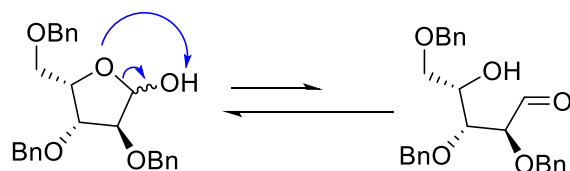
Scheme 7 – Removal of orthogonal protecting group of protected methyl-L-xylofuranoside

2.1.2 Addition of amine-hydroxyl and regiospecific O-silylation to protected methyl-L-xylofuranoside



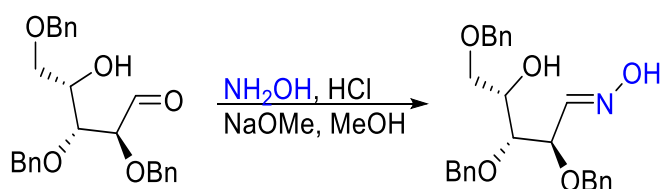
Scheme 8 - Addition of amine-hydroxyl and regiospecific O-silylation to perbenzylated L-xylofuranoside

An equilibrium exists between the cyclic form **5** and linear form **5a** of perbenzylated L-xylose in which the cyclic form is the dominant (**Scheme 9**)



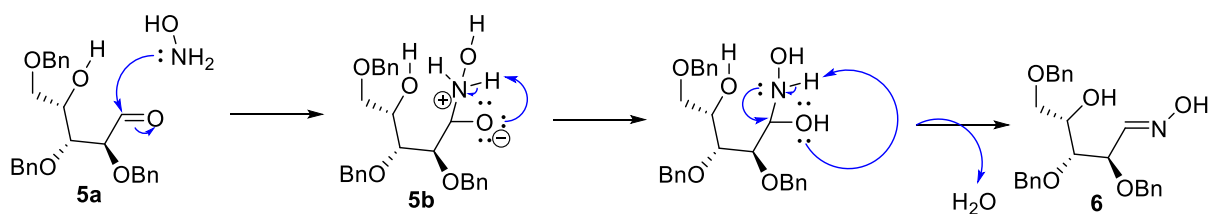
Scheme 9 – Weak equilibrium between cyclic form and linear form

The motivation behind this reaction was to install a nitrogen atom such that one could create *N*-spirofused iminosugar. When the linear form **5a** of perbenzylated L-xylose reacts with hydroxylamine generated *in situ* from hydroxylamine hydrochloride and sodium methoxide ($\text{HONH}_2 \cdot \text{HCl} + \text{NaOMe} \rightarrow \text{NH}_2\text{OH} + \text{NaCl} + \text{MeOH}$), aldoxime **6** is formed. Due to the Le Chatelier's principle, the equilibrium in Scheme 9 shifts towards **5a** as more aldoxime **6** is being formed.



Scheme 10 – Addition of hydroxylamine to aldehyde

The lone pair electrons on the hydroxylamine attacks the carbonyl which readily donates electrons to the oxygen atom meanwhile oxygen deprotonates the quaternary ammonium intermediate **5b**. Oxygen further deprotonates the quaternary ammonium, thereby inducing hydrolysis while newly formed lone pair electrons on the nitrogen atom attacks the carbon and as a result providing oxime **6** (Scheme 11).



Scheme 11 – Suggested mechanism of addition of hydroxylamine to aldehyde

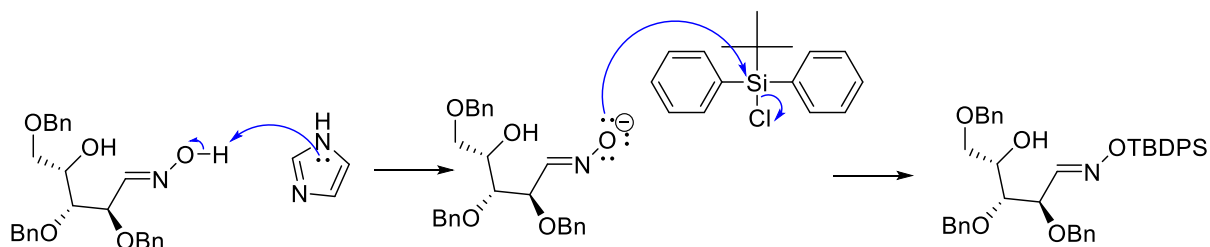
The product was instantly used in the next reaction without further purification and the yield is therefore not disclosed.

The following reaction concerns the regiospecific *O*-silylation of aldoxime **6** due to steric hindrance of the second hydroxyl group. The oxime was treated with tert-butyl diphenylsilyl chloride (TBDPSCl) and imidazole to give the silyl protected oxime **7** and making Cl the leaving group (**Scheme 12**).



Scheme 12 – O-silylation of oxime

The suggested mechanism in **Scheme 13** initiates by deprotonation by the imidazole on the hydrogen in the oxime hydroxyl group, giving oxygen an extra pair of lone electrons. Lone pair electrons on the oxygen atom attacks the silicon atom of TBDPSCl meanwhile the chloride group is expelled thereby forming the protected oxime **7**. It is although uncertain whether the imidazole group deprotonates the oxime before or after *O*-silylation. Oxime **7** was purified by flash silica gel column chromatography (FCC) and provided a yield of 54%.



Scheme 13 – Suggested mechanism of O-silylation of oxime

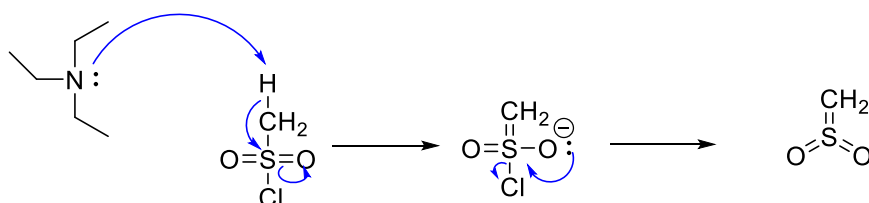
2.1.3 *O*-Mesylation of silyl protected oxime

The motivation behind the synthesis is to create a stereospecific cyclization to create an N-oxime. The hydroxyl group of the silyl protected oxime **7** is a poor leaving group and needs to be substituted by a better leaving group that doesn't constitute to any steric hindrance. Oxime **7** was therefore treated with triethylamine and mesyl chloride to form mesylate **8** (**Scheme 14**).



Scheme 14 – Mesylation of silyl-protected oxime

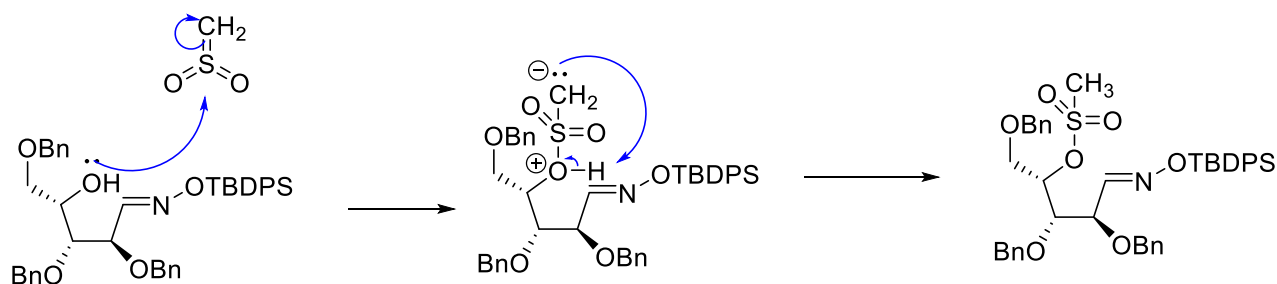
Triethylamine acts as a base and deprotonates the methyl group of MsCl. The carbon atom readily donates electrons to the central sulfur atom which in turn donates to the oxygen atom. Oxygen stabilizes the negative charge by expelling the Cl atom (**Scheme 15**).



Scheme 15 – Suggested mechanism of acid-base reaction between triethylamine and mesylchloride

The oxygen in the free hydroxyl group in compound **7** acts as a nucleophile and attacks the sulfur atom which by further electron transfer stabilization yields mesylate **8** (**Scheme 16**).

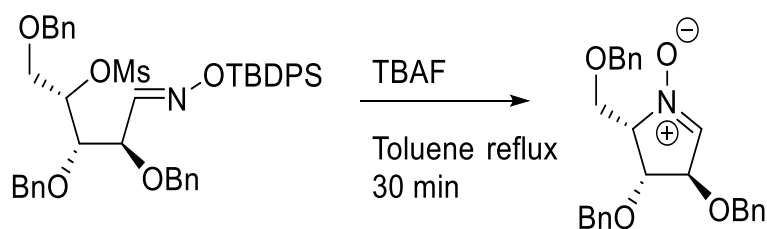
The product was purified by FCC and had a total yield of 74%



Scheme 16 – Suggested mechanism on mesylation of silyl-protected oxime

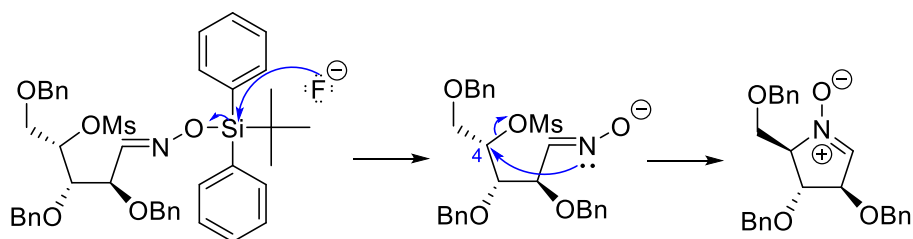
2.1.4 Formation of zwitterionic N-Oxide by addition elimination through pentacoordinated intermediate

To finalize the iminosugar structure, the silyl-protecting group was removed in expectation of a stereospecific cyclization into 5-membered zwitterionic N-oxide compound **9** (**Scheme 17**).



Scheme 17 – Formation of zwitterionic N-oxide

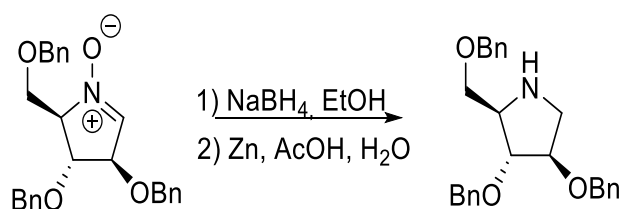
Compound **9** was synthesized by removal of the silyl-protecting group from compound **8** by reaction with TBAF in toluene reflux (**Scheme 17**). After deprotecting, compound **8** was transformed to a reactive intermediate **8a**, which would be due to the nucleophilicity of the nitrogen atom that initiates an intramolecular stereospecific S_N2 substitution to the carbon residing in the 4th position. This would create a pentacoordinated intermediate which would in turn quickly stabilize and form compound **9**, thereby after being subjected to FCC gave a yield of 66% (**Scheme 18**).



Scheme 18 – Suggested mechanism on formation of zwitterionic N-oxide

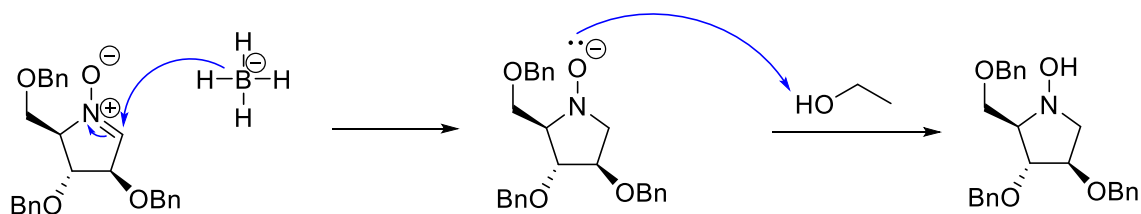
2.1.5 Reduction of N-C double bond by NaBH₄ and Deoxygenation by Zn

The pyrrole-oxide **9** was reduced in a sequence including reduction of N-oxide by NaBH₄ into the corresponding hydroxylamine and reduction of hydroxylamine to the corresponding amine (**Scheme 19**).



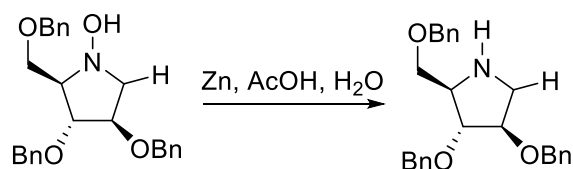
Scheme 19 – Reduction of N-C double bond by NaBH₄ and Zn

Borohydride expels a hydrogen atom which reacts with the double bond of the pyrrole-oxide **9** to initiate an electron rearrangement to eliminate the double bond to form amine-oxide **9a**. Lone pair electrons from the N-oxide oxygen subsequently attack a methanol group to form the hydroxylamine **9b** (Scheme 20).



Scheme 20 - Suggested mechanism on reduction of N-C double bond by NaBH₄

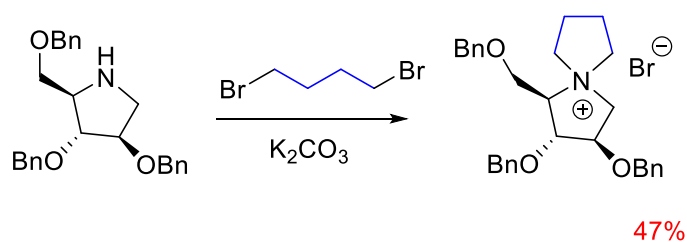
Zn further reduces hydroxylamine **9b** to pyrrolidine **10**, however the mechanism is yet poorly understood (Scheme 21). Product **10** was subjected to FCC and gave a total yield of 70% over two steps (Double bond reduction and deoxygenation).



Scheme 21 - Deoxygenation to primary amine by Zn

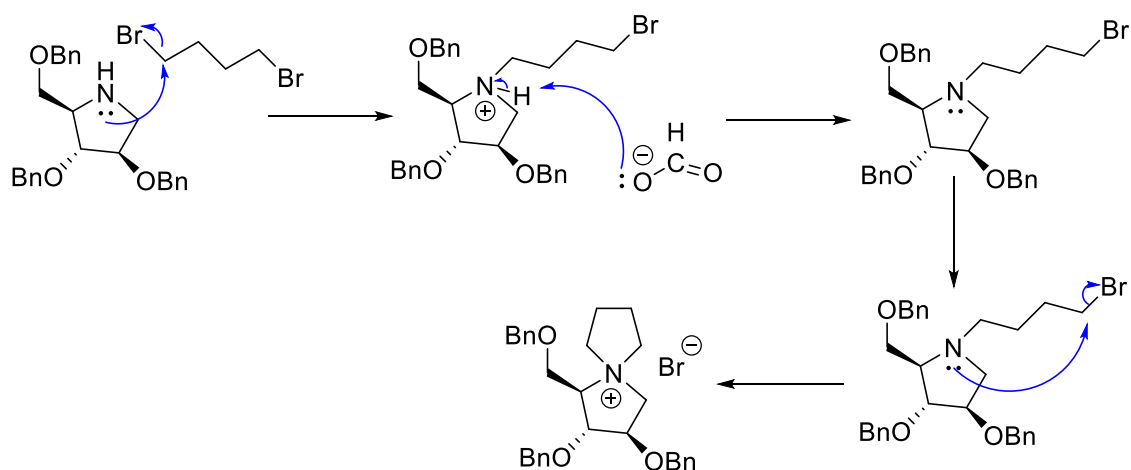
2.1.6 Synthesis of N-spirofused bicyclic iminosugar by double S_N2 substitution

Amine **10** underwent a double S_N2 substitution with 1,4-dibromobutane to afford ammonium bromide **11**, which accommodates a permanent positive charge on the spirocyclic nitrogen atom S_N2 (Scheme 22). The choice of base was determined by the salt that would form after the corresponding reaction. K₂CO₃ was therefore a competent choice for this reaction.



Scheme 22 – Double S_N2 substitution on primary amine

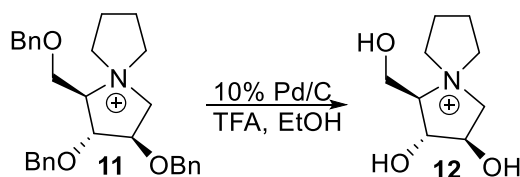
The reaction of compound **10** initiates by a nucleophilic attack by the lone pair electron on the nitrogen atom on the alkyl halide carbon with the lowest electron density. K_2CO_3 proceeds to deprotonate the nitrogen atom, thereby creating a new pair of lone electrons in intermediate **10a** which can initiate a new nucleophilic attack on the tail end of the alkyl halide chain and providing compound **11** (**Scheme 23**). The remaining product was subjected to FCC and gave a total yield of 47%.



Scheme 23 – Suggested mechanism on double S_N2 substitution on primary amine

2.1.7 Benzyl group deprotection of *N*-spirofused iminosugar

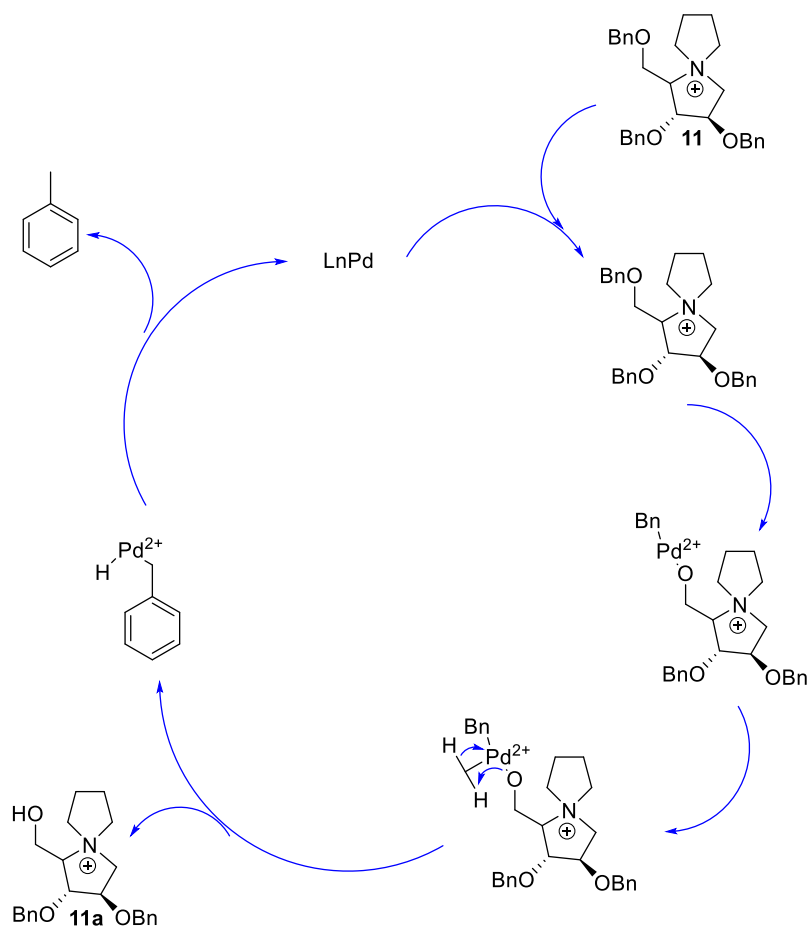
The protected *N*-spirofused bicyclic iminosugar was treated with 10% Pd/C hydrogenation and TFA in ethanol to deprotect the earlier reinstated *O*-Benzylated protecting groups to provide the *N*-spirofused iminosugar **12** (**Scheme 24**).



*Scheme 24 - Deprotection of *N*-spirofused iminosugar*

The deprotection of the *O*-benzyl groups using palladium-on-carbon as a catalyst was further accelerated using TFA in ethanol which readily increases the coordination ability of Pd/C onto the amine.

Pd/C situates itself between the benzylic leaving group and oxygen before hydrogenation initiates. Palladium leaves with the benzyl group thereby giving **11a** with one less protected group. Pd/C is recovered and the reaction restarts providing iminosugar **12** in the end (**Scheme 25**). The final product was filtered through Celite and gave quantitative yield.



Scheme 25 - Suggested mechanism on deprotection of N-spirofused iminosugar²⁹

2.2 Concluding remarks and the future of AChE inhibitors

The *N*-spirofused iminosugar **12** was successfully synthesized as a potential AChE inhibitor from several steps starting with L-xylose, where a Fisher glycosylation method was done before global *O*-benzylation was performed. A nitrogen atom was inserted in the form of hydroxylamine addition before introduction of a silyl protecting group. To produce a good leaving group, the protected oxime was mesylated before removal of the silyl protecting group, thus creating an intramolecular S_N2 substitution through a pentacoordinated intermediate. The pyrrole-oxide was further reduced and deoxygenated to form a protected

pyrrolidine, which was thereby treated with a double substituted alkylhalide that would provide as a strong nucleophile that also wouldn't create steric hindrance and a base that would subsequently not form an interfering salt to provide the protected edition of the *N*-spirofused iminosugar. Furthermore, by using a different solvent when synthesizing compound **11** should be examined as TLC analysis of **11** was suspected of being contaminated by remaining traces of DMF. Alternatively, one could use other aprotic solvents with lower boiling points like acetone or acetonitrile. Finally, **11** was treated with Pd/C in acidic environments to finalize the *N*-spirofused iminosugar. However, treatment of Pd/C hydrogenation in acid for 1 day was not sufficient and would require more time and more acid to accelerate and fulfill the reaction.

We believe that our synthesis strategy would be sufficient in synthesizing bundles of *N*-spirofused ammonium compounds. Further work would have to be done to determine the inhibition effect that compound **12** would provide. Our sample of compound **12** is therefore being sent to associate professor Óscar Lopéz at the University of Seville to test the performance of **12** as an AChE.

3. Experimental

3.1 Practical

3.1.1 Solvents and reagents

The chemicals used were all obtained from Sigma Aldrich, VWR or Merck and used as supplied unless otherwise stated in the experimental protocols.

3.1.2 Spectrometric and spectroscopic analysis

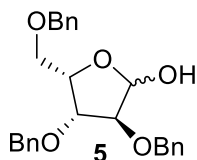
Nuclear magnetic resonance (NMR) spectra were recorded on the Bruker Ascend TM 400 series, operating at 400 MHz for ^1H and MHz for ^{13}C , respectively. The chemical shifts (δ) are expressed in ppm relative to residual CDCl_3 (^1H , 7.26 ppm; ^{13}C , 77.16 ppm), D_2O (^1H , 4.79 ppm) and CD_3OD (^1H , 3.31 ppm; ^{13}C , 49.00 ppm). Coupling constants (J) are given in Hertz (Hz) and the multiplicity is reported as: singlet (s), doublet (d), triplet (t), doublet of doublets (dd), multiplet (m) and broad singlet (bs). The assignments of signals in various NMR spectra were often assisted by conducting heteronuclear single-quantum correlation spectroscopy (HSQC), heteronuclear multiple bond correlation spectroscopy (HMBC) and homonuclear correlated spectroscopy (COSY).

3.1.3 Chromatography

Thin-layer chromatography (TLC) was carried out using aluminium backed 0.2 mm silica gel plates. The spots of the product were detected using ultraviolet (UV) extinction at $\lambda=254$ nm or $\lambda=366$ nm. Flash column chromatography (FC) was also carried out with silica gel, with solvent gradients that are indicated in the procedure. Flash chromatography was carried out with silica gel (particle size 40-63 μm), with solvent gradients as indicated in the experimental procedures.

3.2 Experimental

3.2.1 Methyl 2,3,5-Tri-O-benzyl-L-xylofuranose²⁴



AcCl (0.29mL, 4.0mmol, 0.2 equiv) and L-xylose (3.0g, 20.0 mmol, 1.0 equiv) was added to MeOH (70 mL) which was kept stirring for 2 days in RT. The temperature of the mixture was adjusted to 0°C before NaOH(1M) was added to adjust to pH 10-11. The mixture was evaporated from co-evaporation. The procedure was done three times from toluene (20mL). The remaining product was dissolved in anhydrous DMF (84mL). NaH (60% dispersion in mineral oil (4.61g, 115mmol, 5.75 equiv) was added spoonwise while the mixture was kept stirring in RT under inert gas atmosphere (Ar) for 15 min. The temperature of the mixture was adjusted to 0°C before BnBr (12 ml, 101mmol, 5.05 equiv) was added dropwise to the mixture. The mixture was kept stirring in RT for 1 day. The temperature of the mixture was adjusted to 0°C and H₂O (100mL) was added dropwise. The inorganic solution was extracted by EtoAc (2*100mL) while the organic parts were dried (MgSO₄) and added to a filtered beaker and further evaporated under reduced pressure. The remaining solution was dissolved in 1,4-dioxane (60mL) and aq. HCl (60mL, 4M). The mixture was left stirring at 60-63°C for 2 days suspended in an oil bath. The remaining product was subjected to FCC (Pet.Et, EtoAc 18/2) to yield a yellow syrup (3.16g, 39%)

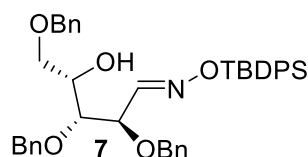
Rf: 0.20 (PE/EtOAc, 3:1 v/v)

¹HNMR CDCl₃, 400 MHz) δ_H: 7.37-7.27 (m, 15H), 5.47 (brs, 1H), 5.23 (d, 1H, J = 6.2 Hz), 4.63 - 4.48 (m, 6H), 4.41-4.37 (m, 1H), 4.10 (dd, 1H, J = 3.1 Hz, J = 5.5 Hz), 4.03 (dd, 1H, J = 2.7 Hz, J = 4.4 Hz), 3.95-3.93 (m, 1H), 3.86 - 3.84 (m, 1H), 3.78 - 3.64 (m, 3H)

¹³CNMR (CDCl₃, 100 MHz) δ_C: 67.2, 68.4, 68.8, 72.0, 72.5, 72.8, 73.2, 73.6, 73.8, 77.4, 77.5, 80.0, 81.2, 81.4, 86.7, 96.4, 101.8, 127.7-128.8 (Ar), 136.9, 137.5, 137.6, 137.7, 137.8, 138.3 (Ar)

11 carbon signals in the sugar region are missing due to signal overlap.

3.2.2 (2R,3R,4S, E)-2,3,5-Tris(benzyloxy)-4-hydroxypentanal O-(tert-butyldiphenylsilylchloride) oxime²⁵



A solution of sodium methoxide (0.69g, 30.1mmol, 10 mL, 4.00 equiv) was added to a solution of **5** (3.16g, 7.75mmol, 1.00 equiv) and hydroxylamine hydrochloride (4.19g, 60.3mmol, 8.00 equiv) in MeOH (45mL). The mixture was left stirring in RT for 1 day and concentrated under reduced pressure. The remaining solids were dissolved in DCM (70mL), purified with distilled water(3x55mL), dried over MgSO₄, filtered, and concentrated under reduced pressure. The remaining yellow syrup was added anhydrous DCM (15mL) and imidazole (0.71g, 10.4mmol, 1.35 equiv) under inert atmosphere (Ar). TBDPSCl (2.81mL, 9.67mmol, 1.25 equiv) was added dropwise while stirring. The mixture was left stirring for 30 min under inert atmosphere (Ar) in RT. The solution was diluted with distilled H₂O/DCM (50mL, 1:1) and was left stirring for 1 day. The organic phase was extracted using DCM (3x55mL). The collection of organic phases was washed with sat. NaCl (25mL), dried over MgSO₄, filtered and concentrated under reduced pressure. The remaining product was subjected to FCC to yield oxime **6** as a colourless syrup (2.84g, 54%).

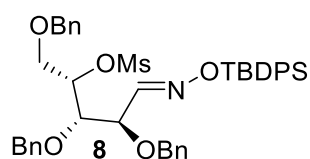
Rf: 0.30 (PE/EtOAc, 19:1, 18:2 v/v)

¹H-NMR (CDCl₃, 400 MHz) δ_H: 7.80 (d, 1H J=8,00Hz) 7.72-7.66 (m, 4H) 7.42-7.20 (m, 21H) 4.63-4.32 (m, 6H) 4.20-3.93 (m, 3H) 3.48-3.30 (m, 3H) 1.10 (s, 9H)

¹³C-NMR (CDCl₃, 100 MHz) δ_C: 20.0, 20.2, 27.6, 27.7, 70.7, 71.5, 71.9, 72.1, 72.3, 72.5, 74.2, 75.2, 75.8, 77.0, 80.6, 81.1, 128.7 -131.0, 134.5, 134.7, 136.7, 138.9, 139.4, 139.5, 156.1, 157.6

3.2.3 2,3,5-Tri-O-benzyl-4-methanesulfonyl-L-xylofuranose

Oxime²⁶



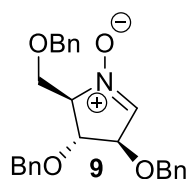
To oxime **6** (2.84g, 4.22 mmol, 1.00 equiv) CH_2Cl_2 (18mL) was added at 0°C under inert atmosphere (Ar). Triethylamine (0.91mL, 6.54mmol, 1.55 equiv) and mesylchloride (0.38mL, 4.94mmol, 1.17 equiv) was added while stirring. The mixture was left stirring for 30 min until water (5mL) was added. The aqueous layer was extracted three times with CH_2Cl_2 (25mL) meanwhile the organic layer was washed with sat. NaCl (25mL), dried over MgSO_4 and concentrated under reduced pressure. The resulting residue was subjected to column chromatography over silica gel (PE, EtOAc 18/2, 17/3) which yielded **7** (2.43g, 74%) as a colourless oil.

Rf: 0.27 (PE, EtOAc, 18/2 v/v)

¹HNMR: (*File corrupted*)

¹³CNMR: (*File corrupted*)

3.2.4 (2R,3R,4R)-3,4-Bis(benzyloxy)-2-((benzyloxy)methyl)-3,4-dihydro-2H-pyrrole 1- oxide²⁵



To a solution of oxime **7** (2.43g, 3.22mmol, 1.00 equiv) anhydrous toluene (50mL) and tert-butyl ammonium fluoride (5mL, 1M in THF, 5 mmol, 1.55 equiv) was added under inert atmosphere (Ar). The reaction was heated to reflux in 45 min before getting cooled to RT. The mixture was diluted with CH_2Cl_2 (50mL). Deionized water (100mL) was added. The aqueous layer was extracted with CH_2Cl_2 (2x75mL) and the organic layers were washed with sat. NaCl (30mL). The impurities were removed by concentrating under reduced pressure.

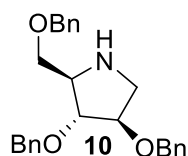
The remaining mixture was subjected to TLC (Hexane/EtoAc, 1/1, 0/1) which yielded **8** (882 mg, 66%) as yellow circular crystals.

Rf: 0.10 (Hexane/EtOAc, 1/1 v/v)

¹H NMR (CDCl₃, 400 MHz) δ_H: 7.30-7.12(m, 15H) , 6.82(5, 1H) , 4.60-4.42(m, 7H), 4.30(dd, 1H, J=2,2Hz, J=3,6Hz) , 4.00-3.93(m 2H), 3.7(dd, 1H, J=3,00Hz , J=10,00Hz)

¹³C NMR (CDCl₃ 100 MHz) δ_C: 66.3, 71.8, 72.0, 73.6, 80.4, 82.8, 127.8-128.7 (Ar), 132.9, 137.3, 137.4, 137.8)

3.2.5- -(2R,3R,4R)-3,4-bis(benzyloxy)-2-[(benzyloxy)methyl]-1H-pyrrolidine²⁷



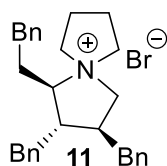
To a solution of **8** (882mg, 2.12mmol, 1.00 equiv), ethanol (55mL) and NaBH₄ (1.605g, 4.24 mmol, 2.00 equiv) was added. The mixture was stirred at RT for 2 days. The resulting crude was subjected to TLC analysis to verify the formation of a new product. Rf = 0.10, Rf_{new} = 0.70. The mixture was added MeOH (3.5mL) and deionized H₂O (10.6mL) and kept stirring under reduced pressure. The newly purified hydroxylamine product was added conc. AcOH (28.3 mL), Zn powder (2.77g, 42.4 mmol, 20 equiv) and deionized H₂O (28.3mL). The mixture was left stirring for 1 day. The mixture was subjected to TLC analysis (DCM: MeOH 30:1) which showed the disappearance of the starting material (Rf = 0.85) and the formation of a new product (Rf = 0.27). The mixture was filtered with cotton, concentrated under reduced pressure. A sat. solution of Na₂SO₄ was added at 0°C to basic pH. The mixture was extracted with EtoAc (3x30mL), where the organic layers were dried over anhyd. Na₂SO₄. The mixture was concentrated under reduced pressure and subjected to Flash Column Chromatography (DCM: MeOH 30:1) which yielded **9** (594mg, 70%) as a yellow oil.

Rf: 0.27 (DCM/MeOH, 30:1 v/v)

¹H NMR (CDCl₃ 400 MHz) δ_H: 7.28-7.21 (m, 15H) 4.47-4.45 (m, 3H) 3.96-3.93 (m, 1H) 3.81-3.80 (m, 1H) 3.56-3.47 (m, 2H) 3.17 (dd, 1H, J=5,20 Hz, J=15,50 Hz) 3.02 (d, 2H J=3,90Hz)

¹³C NMR (CDCl₃ 100 MHz) δ_C: 51.1, 64.2, 70.4, 71.1, 71.9, 73.2, 84.5, 85.8, 127.6-128.4 (Ar) 138.1, 138.3

3.2.6- *-(1R,2R,3R)*-2,3-bis(benzyloxy)-1-[(benzyloxy)methyl]-5-azoniaspiro [4.4] nonane



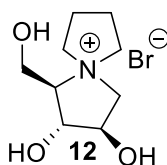
To a solution of **9** (530 mg, 1.27 mmol), DMF (10mL), 1,4-dibromobutane (7.58 mL, 6.35mmol, 5 equiv) and K₂CO₃ (878mg, 6.35 mmol, 5 equiv.) was added. The mixture was left stirring for 1 day. The product mixture was subjected to a TLC analysis (DCM/MeOH 30:1) to confirm the formation of a new product (R_fold = 0.67, R_fnew = 0.53). The mixture was subjected to Flash Column Chromatography (DCM/MeOH 30:1) which yielded product **10** (251 mg, 37%) as white crystals.

R_f: 0.53 (DCM/MeOH 30:1 v/v)

¹HNMR (CD₃OD, 400 MHz) δ_H: 7.37-7.27 (m, 15H) 4.62-4.51 (m, 6H) 4.38 (brs, 1H) 4.30-4.29 (m, 1H) 4.10-4.07 (m, 1H) 4.00-3.81 (m, 5H) 3.74-3.61 (m, 3H) 2.17 (s, 3H)

¹³CNMR (CD₃OD, 100 MHz) δ_C: 20.8, 21.6, 57.0, 59.0, 64.6, 65.6, 66.1, 71.7, 72.0, 73.0, 75.4, 80.0, 82.8, 127.8-128.2 (Ar), 137.0, 137.1

3.2.7 *(1R,2R,3R)*-2,3-Dihydroxy-1-(Hydroxymethyl)-5-azoniaspiro[4.4] nonane²⁴



To **10** (100 mg, 0.109 mmol), 10% Pd/C (100 mg), TFA (8 mL) and EtOH (16mL) was added. The mixture was then subjected under inert atmosphere (Ar) and H₂ gas (1 atm) was introduced. The reaction was left stirring for 1 day. The mixture was filtered through Celite and concentrated under reduced pressure which resulted in the formation of **12** (quantitative yield).

¹HNMR (D₂O, 400 MHz) δ_H: 4.47 (brs, 1H), 4.30 (dd, 1H, *J*=3.70Hz, *J* = 6.90Hz), 3.89-3.59 (m, 9H) 2.26-2.17 (m, 5H)

¹³CNMR (D₂O, 100 MHz) δ_C: 20.4, 21.2, 57.0, 59.2, 66.7, 67.3, 73.6, 76.8, 77.0

References

1. What is alzheimer's?

<https://www.alz.org/alzheimers-dementia/what-is-alzheimers> (accessed March 20, 2022).

2. Alzheimer's Disease International, Dementia Statistics, 2017, Available from

<https://www.alzint.org/about/dementia-facts-figures/dementia-statistics/>, (Accessed 03.05.2022)

3. Norwegian Institute of Public Health, Dementia in Norway, 2015, Available from:

www.fhi.no/en/op/hin/health-disease/dementia-in-norway/, (Accessed 03.05.2022)

4. Statista.com, Norway: Gross domestic product (GDP) in current prices from 1986 to 2026,

Available from:www.statista.com/statistics/327319/gross-domestic-product-gdp-in-norway/, (Accessed 03.05.2022)

5. Breijyeh, Z.; Karaman, R. Comprehensive Review on Alzheimer's Disease: Causes and Treatment. *Molecules* 2020, 25 (24), 5789.

6. Hardy, j. Selkoe, D. The Amyloid Hypothesis of Alzheimer's Disease: Progress and Problems on the Road to Therapeutics. *Science* 2002;297, issue 5580: 353-356

7. Francis PT, Palmer AM, Snape M, et al The cholinergic hypothesis of Alzheimer's disease: a review of progress *Journal of Neurology, Neurosurgery & Psychiatry* 1999;66:137-147.

8. Trang A, Khandhar PB, Physiology, Acetylcholinesterase, Last updated may 2021, Available from: <https://www.ncbi.nlm.nih.gov/books/NBK539735/>, Accessed 04.05.2022

9. Greig, N. H.; Lahiri, D. K.; Sambamurti, K. Butyrylcholinesterase: An Important New Target in Alzheimer's Disease Therapy. *International Psychogeriatrics* 2002, 14 (S1), 77–91.

10. Saxena, A. K. The Structural Hybrids of Acetylcholinesterase Inhibitors in the Treatment of Alzheimer's Disease: A Review. *Alzheimer's & Neurodegenerative Diseases* 2019, 4 (1), 1–25.

11: Marucci, G.; Buccioni, M.; Ben, D. D.; Lambertucci, C.; Volpini, R.; Amenta, F. Efficacy of Acetylcholinesterase Inhibitors in Alzheimer's Disease. *Neuropharmacology* 2021, 190, 108352.

12: National Center for Biotechnology Information. "PubChem Compound Summary for CID 1935, Tacrine" PubChem, <https://pubchem.ncbi.nlm.nih.gov/compound/Tacrine>. (Accessed April 23, 2022.)

13: National Center for Biotechnology Information. PubChem Compound Summary for CID 3152, Donepezil. <https://pubchem.ncbi.nlm.nih.gov/compound/Donepezil>. (Accessed April 23, 2022.)

14: National Center for Biotechnology Information. PubChem Compound Summary for CID 77991, Rivastigmine. <https://pubchem.ncbi.nlm.nih.gov/compound/Rivastigmine>. (Accessed April 23, 2022.)

15: National Center for Biotechnology Information. PubChem Compound Summary for CID 9651, Galantamine. <https://pubchem.ncbi.nlm.nih.gov/compound/Galantamine>. (Accessed April 23, 2022.)

16: National Center for Biotechnology Information. PubChem Compound Summary for CID 4054, Memantine. <https://pubchem.ncbi.nlm.nih.gov/compound/Memantine>. (Accessed April 23, 2022.)

17: Wang, R.; Reddy, P. H. Role of Glutamate and NMDA Receptors in Alzheimer's Disease. *Journal of Alzheimer's Disease* 2017, 57 (4), 1041–1048.

18: Mullard, A. Landmark Alzheimer's Drug Approval Confounds Research Community. *Nature* 2021, 594 (7863), 309–310.

19: Mullard, A. Controversial Alzheimer's Drug Approval Could Affect Other Diseases. *Nature* 2021, 595 (7866), 162–163.

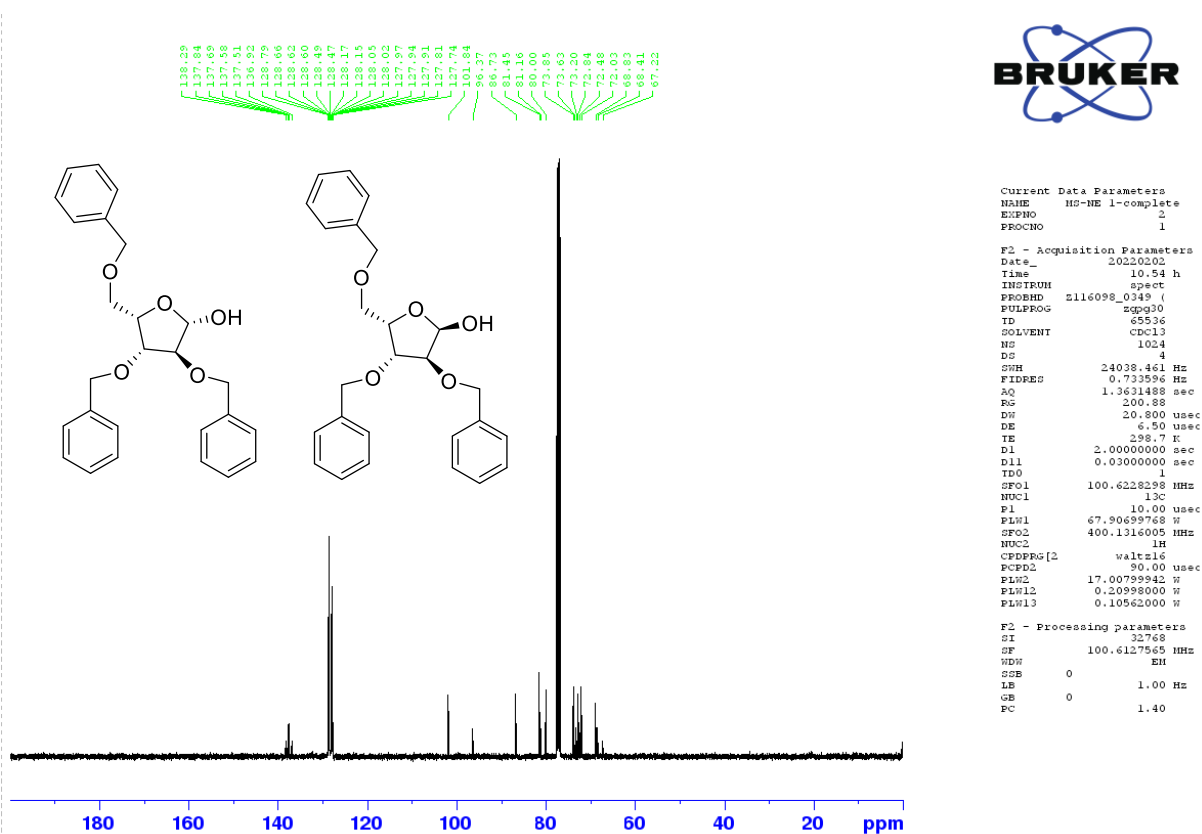
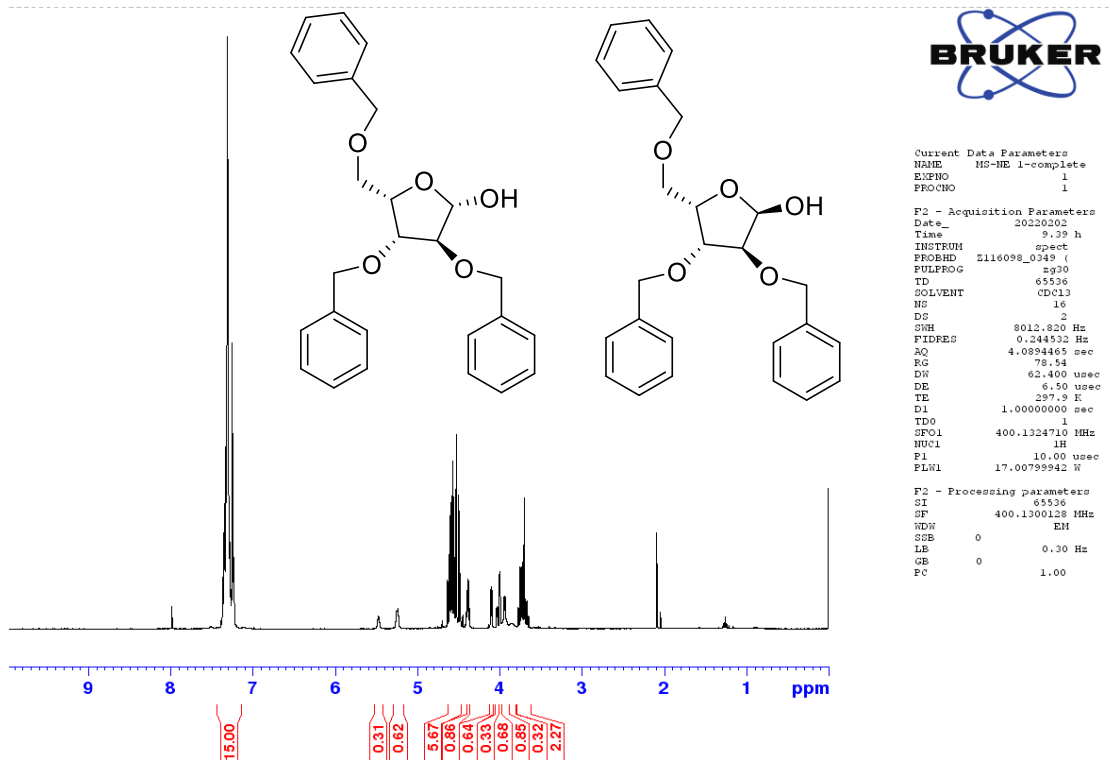
20: Horne, G.; Wilson, F. X.; Tinsley, J.; Williams, D. H.; Storer, R. IMINOSUGARS Past, Present and Future: Medicines for Tomorrow. *Drug Discovery Today* 2011, 16 (3-4), 107–118.

21: e Santana, Q.L.O., T.C.S. Evangelista, P. Imhof, S.B. Ferreira, J.G. Fernández-Bolaños, M.O. Sydnes, Ó. Lopéz, and E. Lindbäck, Tacrine-Sugar Mimetic Conjugates as Enhanced Cholinesterase Inhibitors. *Org. Biomol. Chem.*, 2021. 19, 2322.

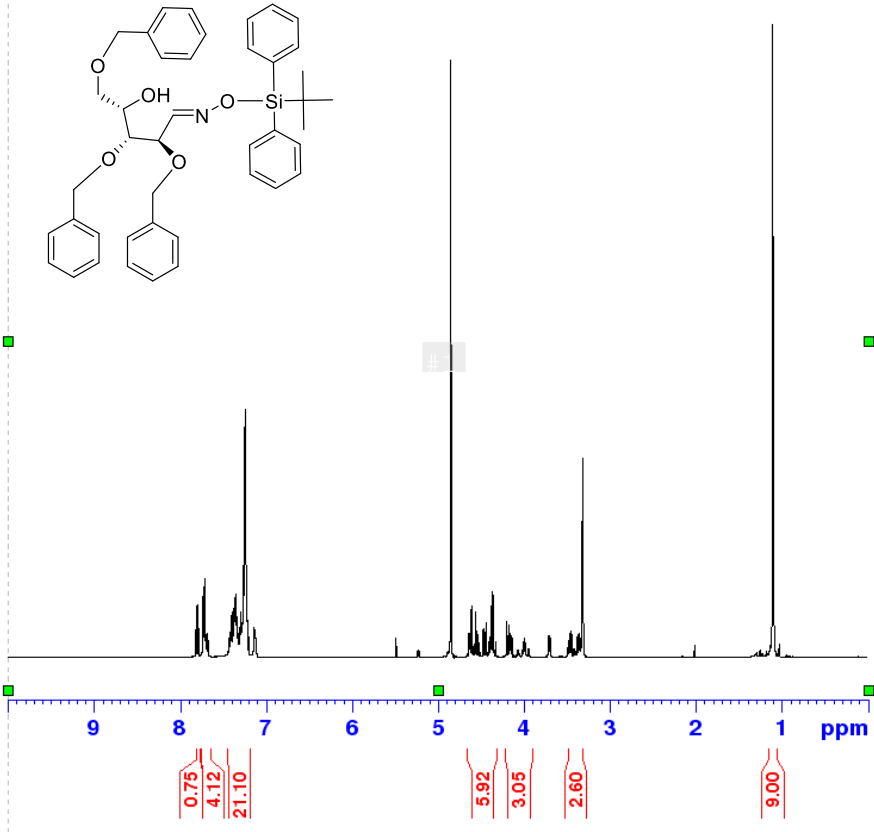
- 22: Sharma, K. Cholinesterase Inhibitors as Alzheimer's Therapeutics (Review). *Molecular Medicine Reports* 2019.
- 23: Memantine: Medlineplus drug information.
<https://medlineplus.gov/druginfo/meds/a604006.html> (accessed May 5, 2022).
- 24: Evangelista, T. C.; Lopéz, Ó.; Sydnés, M. O.; Fernández-Bolaños, J. G.; Ferreira, S. B.; Lindbäck, E. Bicyclic 1-Azafagomine Derivatives: Synthesis and Glycosidase Inhibitory Testing. *Synthesis* **2019**, *51* (21), 4066–4077.
- 25: Rössler, S. L.; Schreib, B. S.; Ginterseder, M.; Hamilton, J. Y.; Carreira, E. M. Total Synthesis and Stereochemical Assignment of (+)-Broussonetine H. *Organic Letters* **2017**, *19* (20), 5533–5536.
- 26: Desvergnés, S.; Py, S.; Vallée, Y. Total Synthesis of (+)-Hyacinthacine A2 Based on Smi2-Induced Nitron Umpolung. *The Journal of Organic Chemistry* **2005**, *70* (4), 1459–1462.
- 27: D'Adamio, G.; Matassini, C.; Parmeggiani, C.; Catarzi, S.; Morrone, A.; Goti, A.; Paoli, P.; Cardona, F. Evidence for a Multivalent Effect in Inhibition of Sulfatases Involved in Lysosomal Storage Disorders (Lsds). *RSC Advances* **2016**, *6* (69), 64847–64851.
- 28: Benzyl Protection of Alcohols. <https://web.jkchemical.com/post/602> (accessed Apr 27, 2022).
- 29: Yang, S. Benzyl deprotection of alcohols. <https://www.jk-sci.com/blogs/resource-center/benzyl-deprotection-of-alcohols> (accessed Apr 26, 2022).
- 30: Pini, L.; Pievani, M.; Bocchetta, M.; Altomare, D.; Bosci, P.; Cavedo, E.; Galluzzi, S.; Marizzoni, M.; Frisoni, G. G. Brain Atrophy in Alzheimer's Disease and Aging. *Ageing Research Reviews* 20q6, 30, 25-48
- 31: Pang, Y.P.; Quiram P.; Jelacic, T.; Hong, F; Brimijoin, S. J. *Biolog, Chem.* 1996, 271, 23646-23649.

Appendix

Methyl 2,3,5-Tri-O-benzyl-L-xylofuranose



(2R,3R,4S, E)-2,3,5-Tris(benzyloxy)-4-hydroxypentanal O-(tert-butylidiphenylsilylchloride) oxime

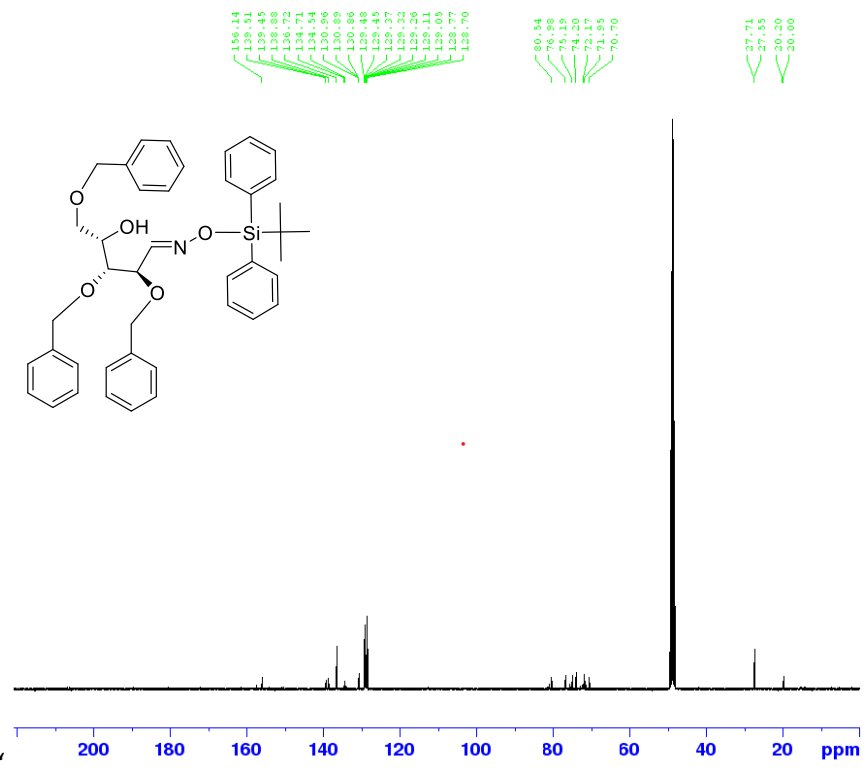


Current Data Parameters
 NAME MS-NE 2
 EXPNO 1
 PROCNO 1

F2 - Acquisition Parameters
 Date_ 20220211
 Time 16.32 h
 INSTRUM spect
 PROBHD Zll6098_0349 ()
 PULPROG zg30
 TD 65536
 SOLVENT MeOD
 NS 16
 DS 2
 SWH 8012.820 Hz
 FIDRES 0.244532 Hz
 AQ 4.0894465 sec
 RG 71.31
 DW 62.400 usec
 DE 6.50 usec
 TE 299.1 K
 D1 1.00000000 sec
 TD0 1
 SFO1 400.1324710 MHz
 NUCL1 1H
 FL 10.00 usec
 PLW1 17.00799942 W

F2 - Processing parameters
 SI 65536
 SF 400.1300077 MHz
 WDW EM
 SSB 0
 LB 0.30 Hz
 GB 0
 PC 1.00

MS-NE BCH 2

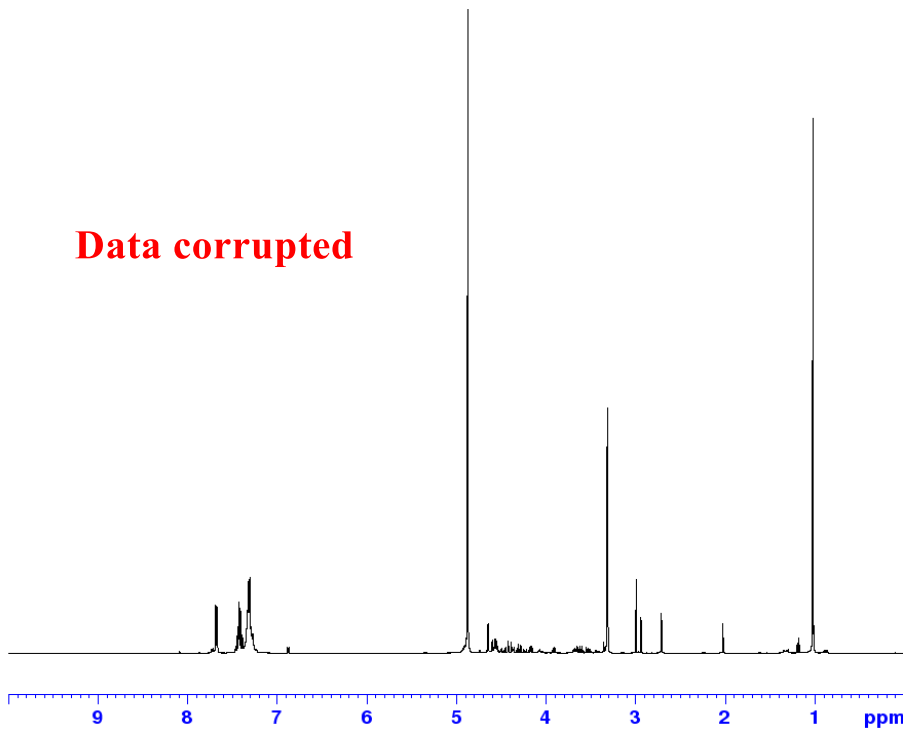


Current Data Parameters
 NAME MS-NE 2
 EXPNO 4
 PROCNO 1

F2 - Acquisition Parameters
 Date_ 20220211
 Time 17.41 h
 INSTRUM spect
 PROBHD Zll6098_0349 ()
 PULPROG zgpg30
 TD 65536
 SOLVENT MeOD
 NS 4
 DS 4
 SWH 24038.461 Hz
 FIDRES 0.733596 Hz
 AQ 1.361488 sec
 RG 200.88
 DW 20.800 usec
 DE 6.50 usec
 TE 299.7 K
 D1 2.00000000 sec
 D11 0.03000000 sec
 TD0 1
 SFO1 100.6228298 MHz
 NUCL1 13C
 FL 10.00 usec
 PLW1 67.90699768 W
 SFO2 400.1316005 MHz
 NUCL2 1H
 CPDPRG2 waltz16
 PCPD 90.00 usec
 PLW2 17.00799942 W
 PLW1L 0.20998000 W
 PLW1J 0.10562000 W

F2 - Processing parameters
 SI 32768
 SF 100.6126292 MHz
 WDW EM
 SSB 0
 LB 1.00 Hz
 GB 0
 PC 1.40

2,3,5-Tri-O-benzyl-4-methanesulfonyl-L-xylofuranose Oxime

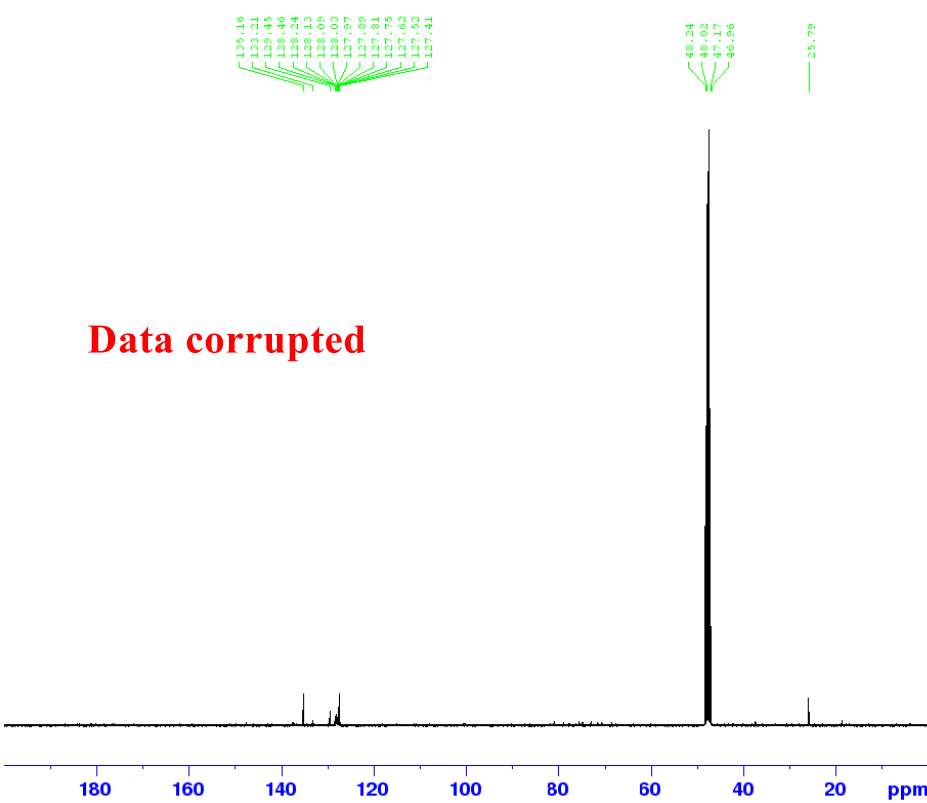


```

Current Data Parameters
NAME      HS-NE 3 V2
EXPNO    1
PROCNO    1

F2 - Acquisition Parameters
Date_     20220325
Time      16:22 h
INSTRUM   spect
PROBHD    Z116098_0349 (
PULPROG   zg30
TD         65536
SOLVENT   MeOD
NS         16
DS         2
SWH        8012.820 Hz
FIDRES     0.244532 Hz
AQ         4.0894465 sec
RG         89.12
DN         62.400 usec
DE         6.50 usec
TE         297.2 K
D1         1.00000000 sec
TDO        1
SFO1      400.1324710 MHz
NUC1       1H
P1         10.00 usec
PLW1      17.00799942 W

F2 - Processing parameters
SI         65536
SF         400.1300069 MHz
WDW        EM
SSB        0
LB         0.30 Hz
GB         0
PC         1.00
    
```



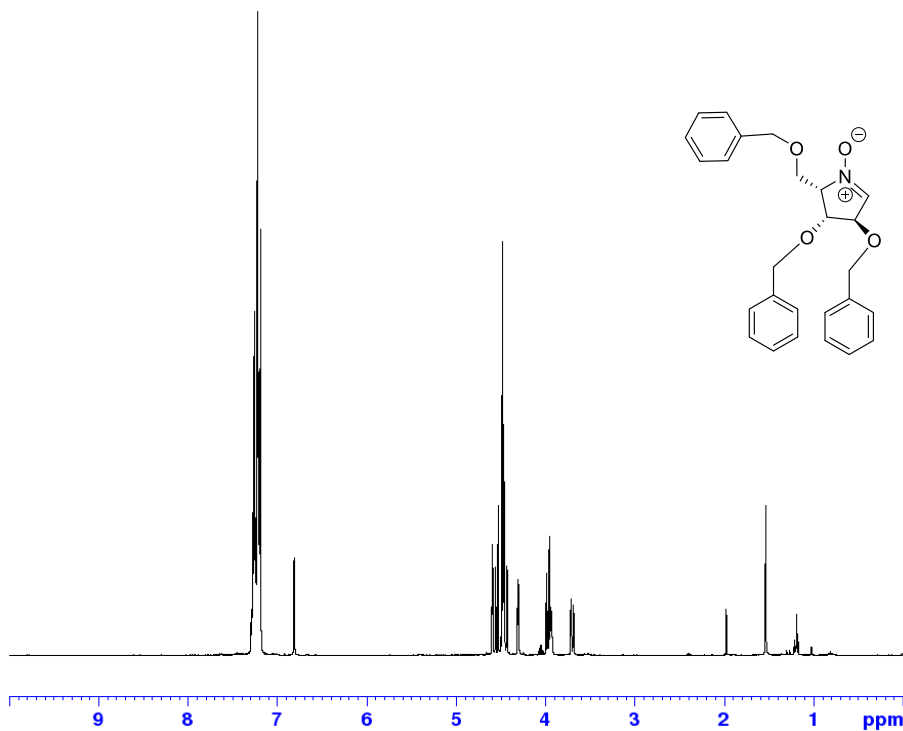
```

Current Data Parameters
NAME      HS-NE 3 V2
EXPNO    2
PROCNO    1

F2 - Acquisition Parameters
Date_     20220325
Time      17:38 h
INSTRUM   spect
PROBHD    Z116098_0349 (
PULPROG   zgpg30
TD         65536
SOLVENT   MeOD
NS         1024
DS         4
SWH        24038.461 Hz
FIDRES     0.733596 Hz
AQ         1.3631488 sec
RG         200.88
DN         20.800 usec
DE         6.50 usec
TE         298.0 K
D1         2.00000000 sec
D11        0.03000000 sec
TDO        1
SFO1      100.6228298 MHz
NUC1       13C
P1         10.00 usec
PLW1      67.90699768 W
SFO2      400.1316005 MHz
NUC2       1H
CPDPRG2   waltz16
PCPD2     90.00 usec
PLW2      17.00799942 W
PLW12     0.20998000 W
PLW13     0.10562000 W

F2 - Processing parameters
SI         32768
SF         100.6127685 MHz
WDW        EM
SSB        0
LB         1.00 Hz
GB         0
PC         1.40
    
```

(2R,3R,4R)-3,4-Bis(benzyloxy)-2-((benzyloxy)methyl)-3,4-dihydro-2H-pyrrole 1-oxide

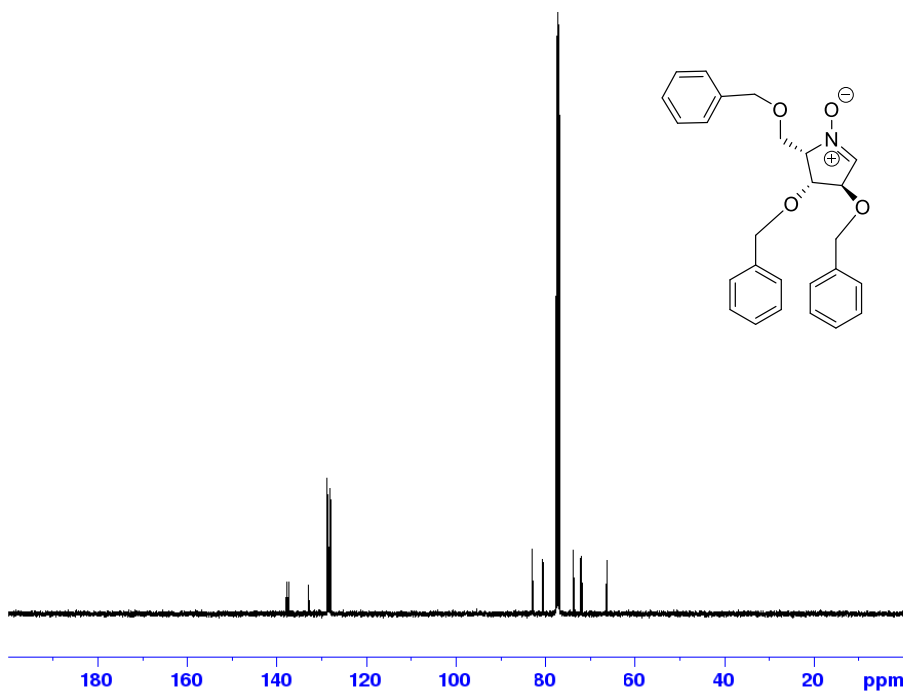
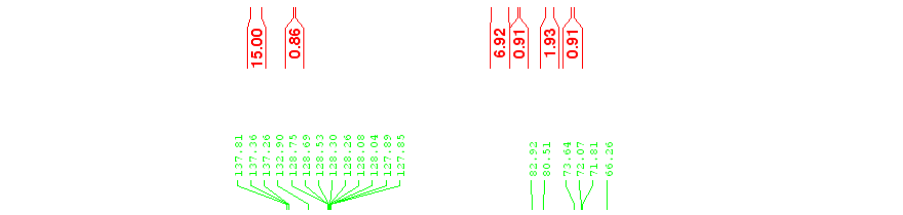


```

Current Data Parameters
NAME      HS-NE 4
EXPNO    1
PROCNO    1

F2 - Acquisition Parameters
Date_    20220223
Time     11.11 h
INSTRUM  spect
PROBHD   E116098_0349 (
PULPROG  zg30
TD        65536
SOLVENT  CDCl3
NS        16
DS        2
SWH       8012.820 Hz
FIDRES    0.244532 Hz
AQ        4.0894465 sec
RG        403.33
DW        62.400 usec
DE        6.50 usec
TE        298.0 K
D1        1.00000000 sec
TD0       1
SFO1      400.1324710 MHz
NUC1      1H
PL1       10.00 usec
PL12      17.00799942 W

F2 - Processing parameters
SI        65536
SF        400.130092 MHz
WDW       EM
SSB       0
LB        0.30 Hz
GB        0
PC        1.00
    
```



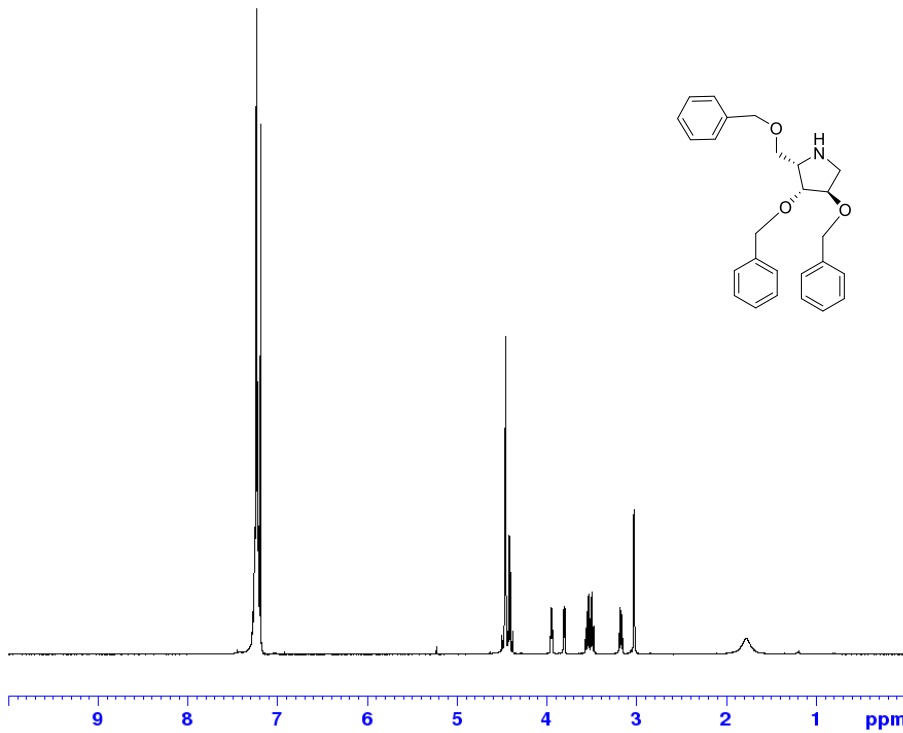
```

Current Data Parameters
NAME      HS-NE 4
EXPNO    1
PROCNO    1

F2 - Acquisition Parameters
Date_    20220223
Time     12.19 h
INSTRUM  spect
PROBHD   E116098_0349 (
PULPROG  zgpg30
TD        65536
SOLVENT  CDCl3
NS        1024
DS        4
SWH       24038.461 Hz
FIDRES    0.733596 Hz
AQ        1.3631488 sec
RG        200.88
DW        20.800 usec
DE        6.50 usec
TE        298.0 K
D1        2.00000000 sec
D11       0.03000000 sec
TD0       1
SFO1      100.6228298 MHz
NUC1      13C
PL1       10.00 usec
PL12      67.90699768 W
SFO2      400.1316005 MHz
NUC2      1H
CPDPRG2  waltz16
PCPD2     90.00 usec
PLW2     17.00799942 W
PLW12    0.20998000 W
PLW13    0.10562000 W

F2 - Processing parameters
SI        32768
SF        100.6127558 MHz
WDW       EM
SSB       0
LB        1.00 Hz
GB        0
PC        1.40
    
```

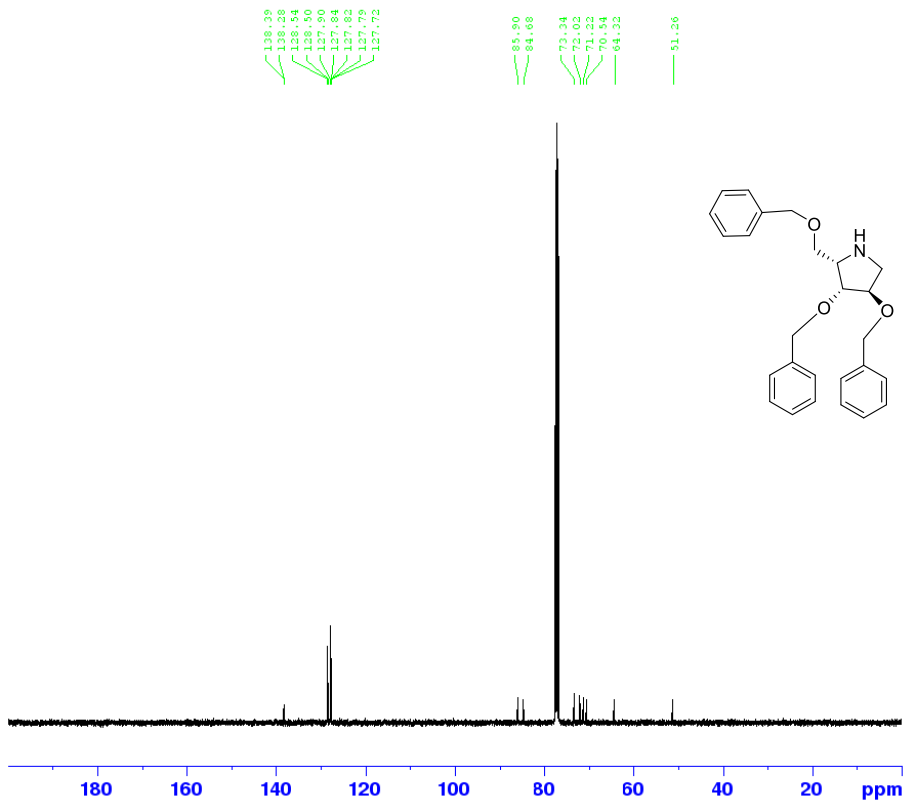
(2R,3R,4R)-3,4-bis(benzyloxy)-2-[(benzyloxy)methyl]-1H-pyrrolidine



Current Data Parameters
 NAME HS-NE 5
 EXPNO 1
 PROCNO 1

F2 - Acquisition Parameters
 Date_ 20220307
 Time 11.30 h
 INSTRUM spect
 PROBHD E116098_0349 ()
 PULPROG zg30
 ID 65536
 SOLVENT CDCl3
 NS 16
 DS 2
 SWH 8012.820 Hz
 FIDRES 0.244532 Hz
 AQ 4.0894465 sec
 RG 117.71
 DW 62.400 usec
 DE 6.50 usec
 TE 297.5 K
 D1 1.00000000 sec
 TD 1
 SF01 400.1324710 MHz
 NUC1 1H
 F1 10.00 usec
 PLW1 17.00799942 W

F2 - Processing parameters
 SI 65536
 SF 400.1300384 MHz
 WDW EM
 SSB 0
 LB 0.30 Hz
 GB 0
 PC 1.00

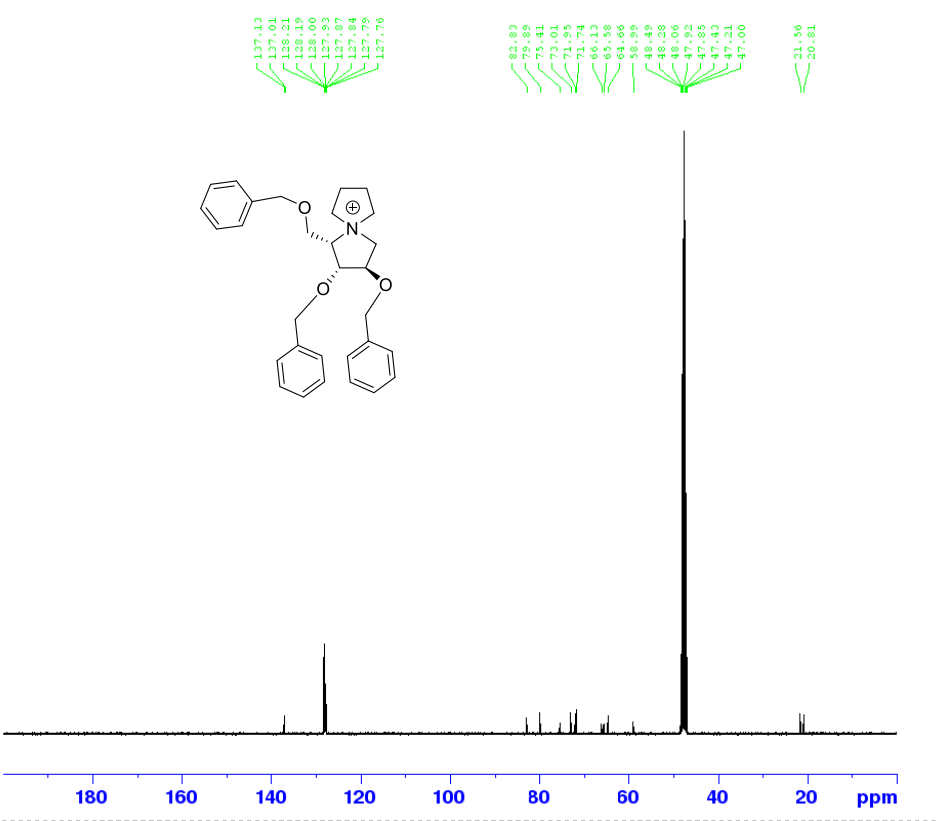
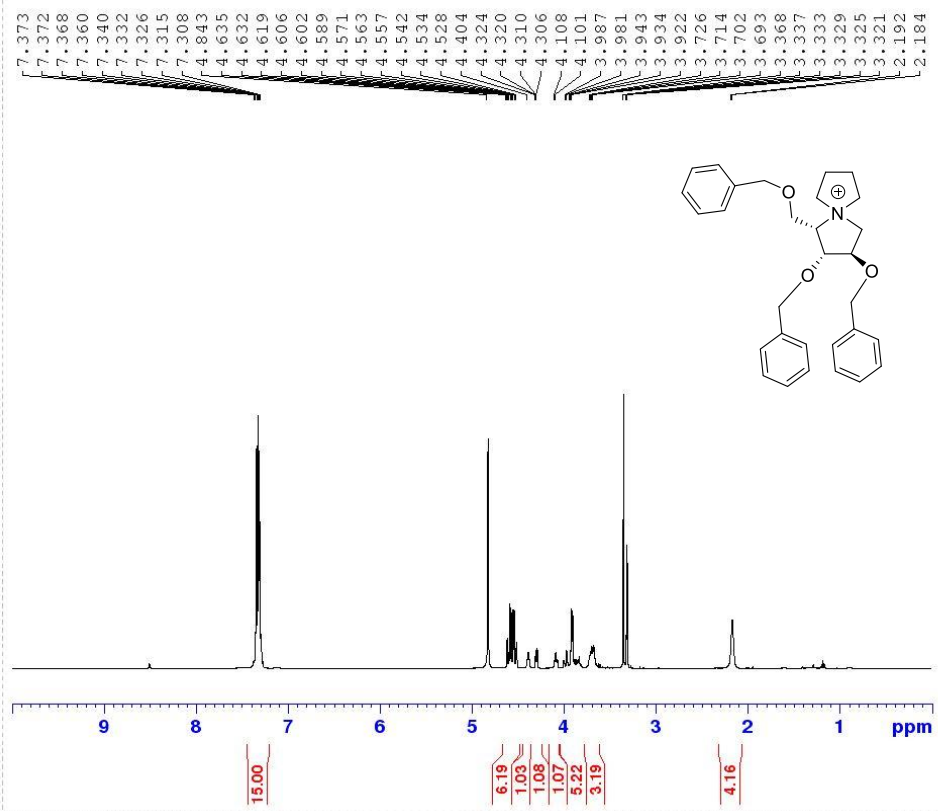


Current Data Parameters
 NAME HS-NE 5
 EXPNO 2
 PROCNO 1

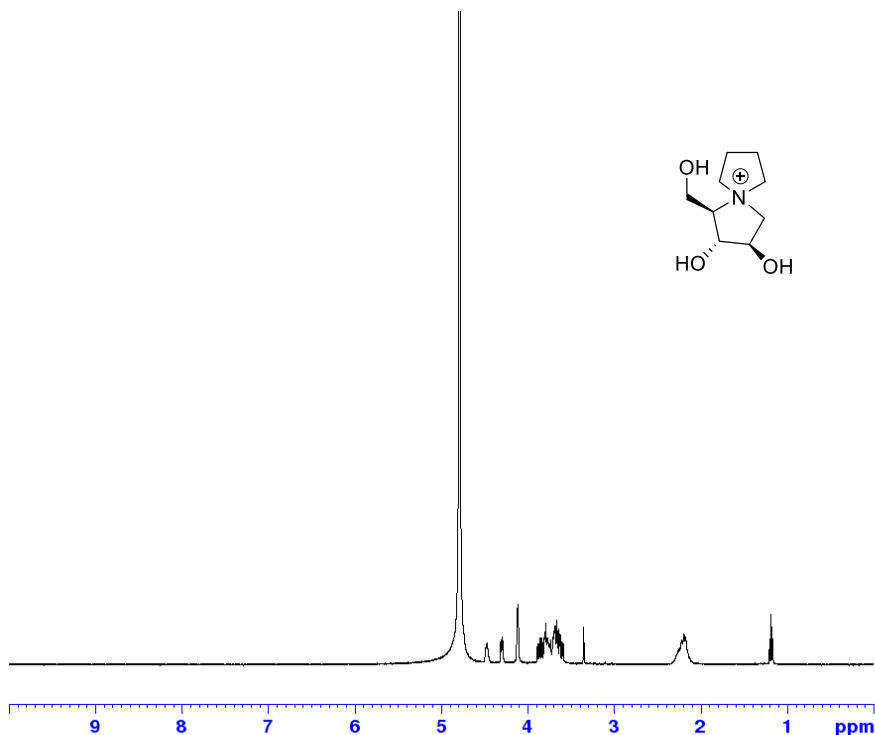
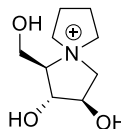
F2 - Acquisition Parameters
 Date_ 20220307
 Time 12.39 h
 INSTRUM spect
 PROBHD E116098_0349 ()
 PULPROG zgpg30
 ID 65536
 SOLVENT CDCl3
 NS 1024
 DS 4
 SWH 24038.461 Hz
 FIDRES 0.733596 Hz
 AQ 1.361188 sec
 RG 200.88
 DW 20.800 usec
 DE 6.50 usec
 TE 298.3 K
 D1 2.00000000 sec
 D11 0.03000000 sec
 TD 1
 SF01 100.6228298 MHz
 NUC1 13C
 F1 10.00 usec
 PL11 67.90699763 W
 SF02 400.1316005 MHz
 NUC2 1H
 CPDPRG2 waltz16
 PCPD2 90.00 usec
 PL12 17.00799942 W
 PLW12 0.20998000 W
 PLW13 0.10562000 W

F2 - Processing parameters
 SI 32768
 SF 100.6127549 MHz
 WDW EM
 SSB 0
 LB 1.00 Hz
 GB 0
 PC 1.40

(1*R*,2*R*,3*R*)-2,3-bis(benzyloxy)-1-[(benzyloxy)methyl]-5-azoniaspiro [4.4] nonane



(1R,2R,3R)-2,3-bis(benzyloxy)-1-[(benzyloxy)methyl]-5-azoniaspiro [4.4] nonane

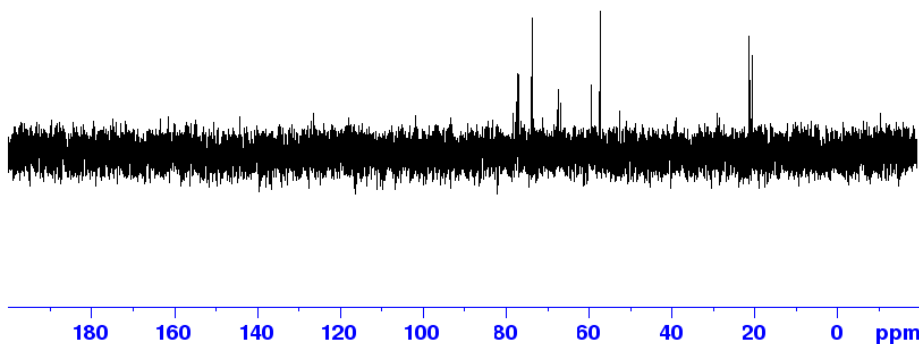
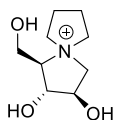


```

Current Data Parameters
NAME      HE-MS HMRP
EXPNO    1
PROCNO    1

F2 - Acquisition Parameters
Date_     20220512
Time      14.03 h
INSTRUM   spect
PROBHD    Z116098_0348 (
PULPROG   zg30
TD         65536
SOLVENT   D2O
NS         16
DS         2
SWH        8012.820 Hz
FIDRES     0.244532 Hz
AQ         4.058485 sec
RG         144
DN         62.400 usec
DE         6.50 usec
TE         298.0 K
D1         1.00000000 sec
TDO        1
SFO1      400.1324710 MHz
NUC1       1H
P1         10.00 usec
PL1        17.00799942 W

F2 - Processing parameters
SI         65536
SF         400.1324710 MHz
WDW        EM
SSB        0
LB         0.30 Hz
GB         0
PC         1.00
    
```



```

CURRENT DATA PARAMETERS
NAME      HE-MS HMRP
EXPNO    2
PROCNO    2

F2 - Acquisition Parameters
Date_     20220512
Time      14.03 h
INSTRUM   spect
PROBHD    Z116098_0348 (
PULPROG   zgpg30
TD         65536
SOLVENT   D2O
NS         16
DS         2
SWH        24033.824 Hz
FIDRES     0.733392 Hz
AQ         1.323280 sec
RG         288.00
DN         28.000 usec
DE         2.10 usec
TE         298.0 K
D1         2.00000000 sec
TDO        0.00000000 sec
SFO1      100.6225294 MHz
NUC1       13C
P1         16.00 usec
PL1        27.00209724 W
PL2        800.1324710 MHz
PL3        16.00 usec
PL4        17.00799942 W
PL5        0.28991880 W
PL6        0.48720800 W

F2 - Processing parameters
SI         65536
SF         100.6225294 MHz
WDW        EM
SSB        0
LB         1.00 Hz
GB         0
PC         1.40
    
```

